Classifying Launch/Impact Events of Mortar and Artillery Rounds Utilizing DWT Derived Features and Feedforward Neural Networks

Myron E. Hohil[1], Sachi Desai[1], and Amir Morcos[1]
[1]US Army RDECOM
Picatinny Arsenal, NJ 07806
USA

mhohil@pica.army.mil; sdesai@pica.army.mil; amorcos@pica.army.mil;

ABSTRACT

Feature extraction methods based on the discrete wavelet transform (DWT) and multiresolution analysis are used to develop a robust classification algorithm that reliably discriminates between launch and impact artillery and/or mortar events via acoustic signals produced during detonation. Distinct characteristics are found within the acoustic signatures since impact events emphasize concussive and shrapnel effects, while launch events are similar to explosions, designed to expel and propel artillery round from a gun. The ensuing blast waves are readily characterized by variations in the corresponding peak pressure and rise time of the waveform, differences in the ratio of positive pressure amplitude to the negative amplitude, variations in the prominent frequencies associated with the varying blast events and variations in the overall duration of the resulting waveform. Unique attributes can also be identified that depend upon the properties of the gun tube, projectile speed at the muzzle, and the explosive/concussive properties associated with the events. In this work, the discrete wavelet transform is used to extract the predominant components and distinct characteristics from the aforementioned acoustic signatures at ranges exceeding 1km. The resulting time-frequency decomposition of the acoustic transient signals is used to produce a separable feature space representation. Highly reliable classification is achieved with a feedforward neural network classifier trained on a sample space derived from the distribution of wavelet coefficients and higher frequency details found within different levels of the multiresolution decomposition. The neural network developed herein provides a capability to classify events (as either launch (LA) or impact (IM)) with a high level of reliability.

1. INTRODCUTION

A network of acoustic sensors can be used to detect and localize artillery launch and/or impact events, and can provide a capability to classify the types of events that have occurred in a specified region provide both warning and identification of threats found in the area. The added information integrated into the common operating picture would assist field commanders to (more) accurately plan and execute measures that must be taken in order to ensure the proper actions for a mission. Such a warning system would also help reduce the time-consuming, manpower intensive and dangerous tasks associated with identifying the events, allowing a field commander to make rapid and accurate judgments that insure greater safety and minimize danger for the soldiers.

The reliability associated with using acoustic sensor technologies to discriminate between artillery events (i.e. launches or impacts) using features that remain robust over long-range wave propagation, firing time, and detonation point (air/ground) are developed and discussed herein. The results described are based on an analysis conducted using acoustic signature data collected during a data collection exercise in the Spring of 2005. The artillery blast data was collected at YUMA Proving Ground (YPG) on 07-11 March

Hohil, M.E.; Desai, S.; Morcos, A. (2006) Classifying Launch/Impact Events of Mortar and Artillery Rounds Utilizing DWT Derived Features and Feedforward Neural Networks. In *Battlefield Acoustic Sensing for ISR Applications* (pp. 25-1 – 25-14). Meeting Proceedings RTO-MP-SET-107, Paper 25. Neuilly-sur-Seine, France: RTO. Available from: http://www.rto.nato.int/abstracts.asp.

Report Documentation Page

Form Approved
OMB No. 0704-0188

1. REPORT DATE	2. REPORT TYPE	3. DATES COVERED
01 OCT 2006	**N/A**	**-**

4. TITLE AND SUBTITLE	5a. CONTRACT NUMBER
Classifying Launch/Impact Events of Mortar and Artillery Rounds Utilizing DWT Derived Features and Feedforward Neural Networks	5b. GRANT NUMBER
	5c. PROGRAM ELEMENT NUMBER
6. AUTHOR(S)	5d. PROJECT NUMBER
	5e. TASK NUMBER
	5f. WORK UNIT NUMBER
7. PERFORMING ORGANIZATION NAME(S) AND ADDRESS(ES) **US Army RDECOM Picatinny Arsenal, NJ 07806 USA**	8. PERFORMING ORGANIZATION REPORT NUMBER
9. SPONSORING/MONITORING AGENCY NAME(S) AND ADDRESS(ES)	10. SPONSOR/MONITOR'S ACRONYM(S)
	11. SPONSOR/MONITOR'S REPORT NUMBER(S)

12. DISTRIBUTION/AVAILABILITY STATEMENT
Approved for public release, distribution unlimited

13. SUPPLEMENTARY NOTES
See also ADM202421., The original document contains color images.

14. ABSTRACT

15. SUBJECT TERMS

16. SECURITY CLASSIFICATION OF:			17. LIMITATION OF ABSTRACT	18. NUMBER OF PAGES	19a. NAME OF RESPONSIBLE PERSON
a. REPORT	b. ABSTRACT	c. THIS PAGE			
unclassified	**unclassified**	**unclassified**	**UU**	**49**	

Standard Form 298 (Rev. 8-98)
Prescribed by ANSI Std Z39-18

2005 in a field test experiment conducted by the Acoustic Center of Excellence (ACOE) from ARDEC (Picatinny Arsenal). The purpose of the experiment was to gather artillery and mortar data and subsequently investigate whether launch events could be distinguished from impact events using acoustic sensor technologies. The field test included the launch and detonation of several variants of artillery, comprising of Type E and Type F rounds and included mortars, Type A, Type B, and Type C; High Explosive (HE) variants. The data set comprised of 52 IM event signatures and 125 LA event signatures collected using microphones emplaced at two sensors sites, S1 and S2, shown in Figure 1. S1 was located approximately 300m from the firing position, while S2 was emplaced 1000m from the firing position and 700m from the impact zone.

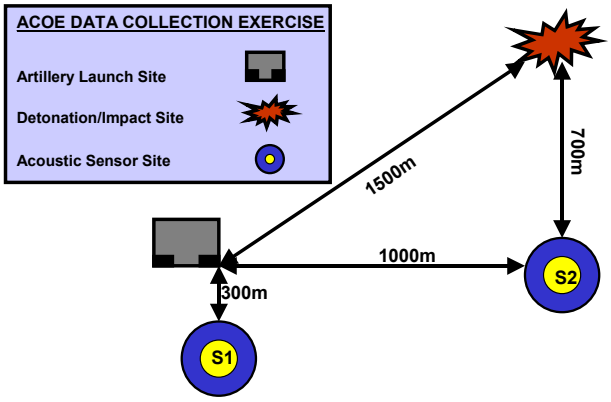

Figure 1 –Layout of Sensor Emplacement at Yuma Proving Grounds for Data Collection 1.

Figure 2 shows three typical acoustic signatures for launches and impacts from various ranges to the sensors. The most notable attributes within each type of blast are readily identified. High frequency precursors that occur prior to the main blast of an IM type event are shown in Figure 2b. These precursors are attributed to various explosive and concussive properties within the blast, which degrade with long-range propagation. Note that the high frequency precursors are absent prior to the main blast as shown in Figure 2a, and 2c. In this work, we identify range invariant features found within the multiresolution decomposition of the corresponding signatures in an attempt to further promote disparate sensor technology for artillery event discrimination. The subsequent development of a feature space representation for classification is based upon data obtained during the YPG data collection exercise in March of 2005. We show that details extracted via different levels of decomposition produce repeatable properties that can be processed and combined to ensure reliable discrimination between these events with various caliber of artillery at varying ranges.

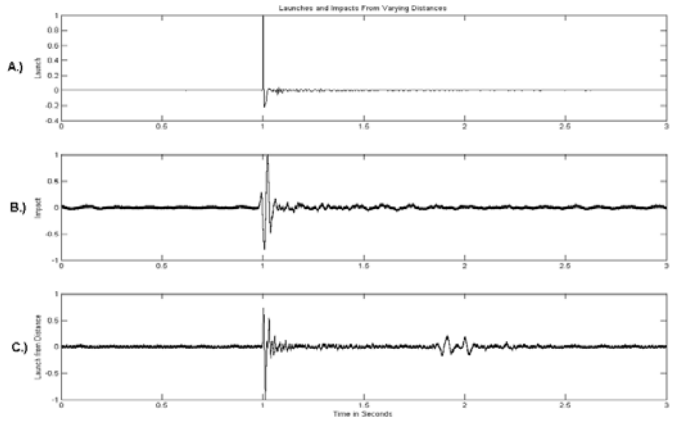

Figure 2 – Acoustic Signatures from YPG (a) Type B launch recorded at S1, (b) Type B impact recorded from S2, (c) Type B launch recorded at S2.

2. WAVELET FEATURE EXTRACTION FOR CLASSIFICATION

Wavelets are used as a basis to identify distinct, disjoint feature sets that remain consistent for a given class of round, and do not degrade dramatically with long-range propagation. The complex, non-stationary response of the signatures to be analyzed, which are categorically poor candidates for feature extraction and segmentation via Fourier analysis or the short-time Fourier Transform. On the other hand, the non-stationary, transient and often oscillatory nature of these signals is well represented with wavelet bases that effectively capture the time-frequency distribution of such signal components. Wavelets are better suited for analyzing transient signals, as they are well localized in time and in frequency, and are able to accommodate the scale of multiple signal components [5]. The wavelet transform can provide a scalable time-frequency representation of artillery blast signatures and can uncover details that are not readily found using conventional signal processing techniques. Noise components introduced into the blasts waves prior to being received at the sensor are a serious impediment to identifying and isolating features that can be used to efficiently characterize the signal. One useful feature of employing wavelets in multiresolution analysis is that this noise can be extracted from the baseband signal of interest; a process referred to as wavelet denoising. Wavelet denoising is optimal in the sense that noise components are removed from the signal components regardless of the frequency content of the signal, which is by far more efficient than conventional filtering methods that retain baseband signal components and suppress high frequency noise.

2.1 DISCRETE WAVELET TRANSFORM AND MULTIRESOLUTIONAL ANALYSIS

The discrete wavelet transform (DWT) is derived from subband filters and is based on a multiresolution decomposition of a signal to give a coarser and coarser approximation to the original signal by removing high frequency detail at each level of decomposition [4]. In other words, the wavelet transform is a multiresolution transform that maps low frequency information of signals into a coarsely sampled subspace and maps high frequency information into more finely sampled subspaces. The DWT is defined by the scaling function

$$\phi(x) = 2^{1/2} \sum_{k=0}^{L-1} h_{k+1} \phi(2x - k) \qquad (1)$$

and a wavelet function

$$\psi(x) = 2^{1/2} \sum_{k=0}^{L-1} g_{k+1} \phi(2x - k) \qquad (2)$$

where h_k and g_k are analysis filters. Choosing the appropriate wavelet filter is important in retaining the characteristics of the transient signals in question. The quality of wavelet decomposition depends significantly on the ability to approximate the signal with wavelets, so the choice of the wavelet scaling function should have properties similar to the original signal. The output of the wavelet transform shows the correlation between the signal and wavelet as a function of time. The easiest method for choosing a wavelet is to copy a signal's time-frequency behavior, however, most transient signals cannot be used as wavelet basis functions since they resemble exponentially damped sinusoids and do not possess a zero mean.

The wavelet basis used in this paper is the db4 and db7 wavelet defined by Daubechies [3] that has the scaling function shown in Figure 3(a) and 3(c) for both Daubechies Wavelets. The translation function is shown in Figure 3(b), and 3(d) respectively for each of the wavelets. Note that scaling function closely resembles the blast signature of the artillery launch and artillery impact acoustic waves shown in Figure 2a and 2b, as well as the acoustic signature found in Figure 2c.

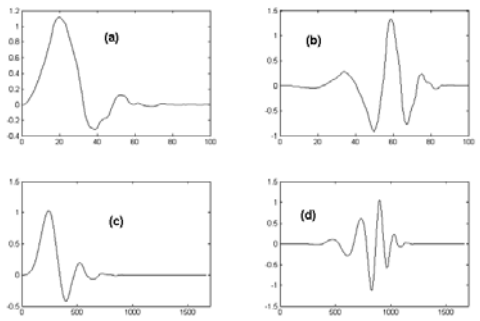

Figure 3 – Daubechies wavelet (a) j = 4 Scaling Function, (b) j = 4 Translation Function, (c) j = 7 Scaling Function, (d) j = 7 Translation Function

The multiresolution filter bank shown in Figure 4 is used to implement the DWT using low pass and high pass wavelet filters to decompose an input signal into different frequency bands. At each level of decomposition, the high pass filter defined in (b, d) produces the detail information, D_j, while the low pass filter associated with the scaling function in (a, c) produces the coarse approximations A_j. The process of successive lowpass and high pass filtering of the input signal to implement the DWT is often referred to as the Mallat algorithm as described in [5]. The resulting banks of dyadic multirate filters are used to split up the input signal's frequency components into different subbands at each decomposition level, each with a subset of frequencies spanning half of the original frequency band. If the original signal is sampled at a frequency of f_S Hz, then the output of the first high pass filter, which is the first detail coefficient D_1, captures the band of frequencies between $f_S/2$ and $f_S/4$. This doubles the frequency resolution as the uncertainty in frequency is reduced by a factor of 2. In the same fashion, the highpass filter in the second stage would capture signal components with a bandwidth between $f_S/4$ and $f_S/8$, and so on. In this way, an arbitrary resolution in frequency can be obtained. Since the input signal at each stage of decomposition contains the highest frequency equivalent to twice that of the output stages, it can

be sampled at half the original sampling frequency, thus discarding half the samples with no loss of information. This decimation by 2, halves the time resolution of the entire signal as the input signal is represented by half of the total number of samples and effectively doubles the scale.

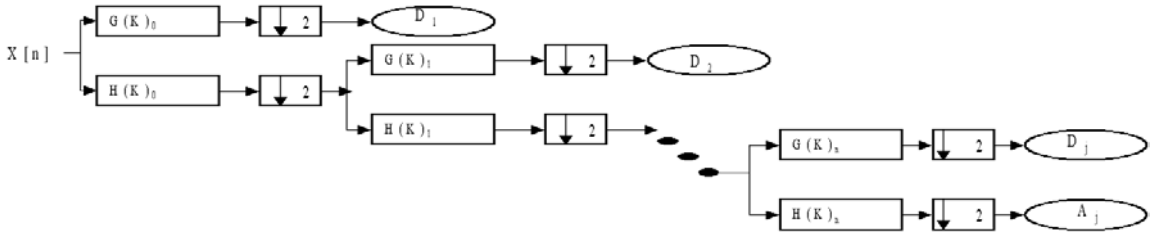

Figure 4 – A Multirate Filter Bank used as a J-Level Wavelet Decomposition Tree.

2.2 WAVELET BASED FEATURES FOR CLASSIFICATION

Figures 5(a-c) show blast waves from two distinct artillery events at various ranges followed by the two signals derived from the multiresolution decomposition shown in Figure 4. The coefficients at level 4 represent the baseband signal and are processed with a db4 wavelet. The details of the signals are the result of a level 7 decomposition using a db7 wavelet. The feature space proposed is comprised of primitives derived from the normalized energy distributions within the details at level 7 and the normalized original signature, centered about the maximum value of the blast wave that results in various power distributions characteristic to the event. In addition, other features are obtained from frequency components derived using a db4 wavelet decomposition. Features such as the rise time for the blast wave and the low frequency content found within the acoustic signals is least attenuated over long propagation distances when compared to some of the predominant features initially identified for discrimination. Plots of the decomposed signals using varying wavelets and feature extraction methods (cf. Figure 5) yield differences that become visible with the varying energy distribution found within the events, including the energy distributions within the precursors of an impact event that are typically absent within launch events. Furthermore, these features are not amplitude dependant as the baseband signal is filtered by the scaling function and only the high-frequency noise components are captured within the details after decomposition.

Let f_p denote the position of the maximum frequency found in the A4 subband after decomposition of the normalized signature utilizing the db4 wavelet [3]. Let A denote the frequencies contained in the subband of A4 and define $\mathrm{B} = \mathrm{A} \geq x\left(A\left(f_p\right)\right)$ where x a threshold used to identify the prominent frequency components found within the A. The count for the total number of prominent frequencies gives the total number of elements in B;

$$F = \text{ Number of elements in B} \quad (3)$$

Let t_p denote the position where the maximum peak overpressure of the normalized signature occurs. Let x denote the threshold of the blast wave, S(t), defined as a percentage of the maximum peak according to $S_p = S \geq x\left(S\left(t_p\right)\right)$ The resulting subset of peaks identify the existence of an initial peak prior to the main blast event;

$$S_{p1} = S_p(1) \quad (4)$$

Let t_m denote the position where the minimum peak underpressure of the normalized blast signature occurs. We define the feature $S_k \in \Re^k$ as the ratio;

$$S_k = \frac{S(t_p)}{S(t_m)} \qquad (5)$$

Let t_b denote the position of the start of the blast event of the normalized signature where the overpressure of the blast wave begins. Let t_c denote the position of the crossing point between the overpressure and underpressure for the normalized signal. Let t_e denote the position of the end of the blast event of the normalized blast wave. Define the width of the overpressure as $d_k^+ = t_c - t_b$ and the width of underpressure as $d_k^- = t_e - t_c$. We then define the ratio;

$$X_k = \frac{d_k^-}{d_k^+} \qquad (6)$$

Let t_S denote the position of the start of the normalized signature S(t) and t_A denote the position at the end. Let $m = t_s \ldots t_{b-1}, t_b$ denote the positions prior to the main blast event and let $n = t_e \ldots t_{A-1}, t_A$ denote the positions after the main blast. An artificial threshold y is applied to the decomposed signature A to create disjoint subsets $C_k^+ = A \geq y(A(m))$, and $C_k^- = A \geq y(A(n))$. Then D_k^+, D_k^- represent the corresponding number of element in C_k^+ and C_k^- respectively. We then define the feature;

$$Y_k = \frac{D_k^+}{D_k^-} \qquad (7)$$

Let α denote a nominal position prior to t_b of the normalized signature S(t). The final feature found by computing the area of the high frequency precursors according to;

$$E_t = \int_{t_b - \alpha}^{t_b} S \qquad (8)$$

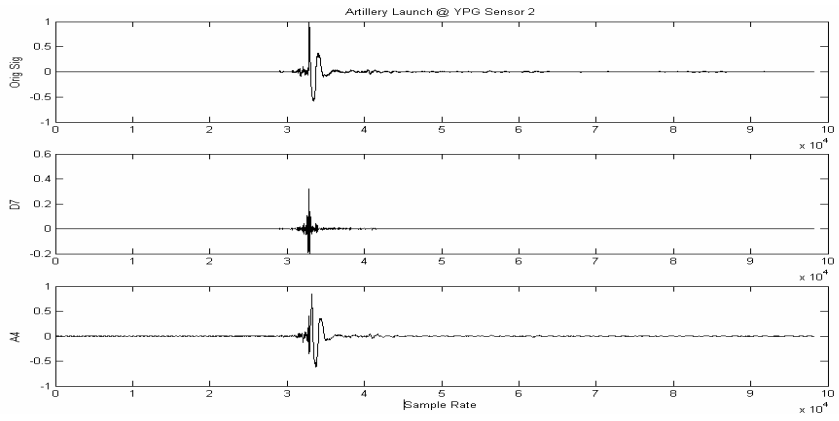

Figure 5a - Artillery Impact Signal and Wavelet Decomposition using db7 and db4 to produce details at level 7 and approximations coefficients at level 4 from Sensor 2.

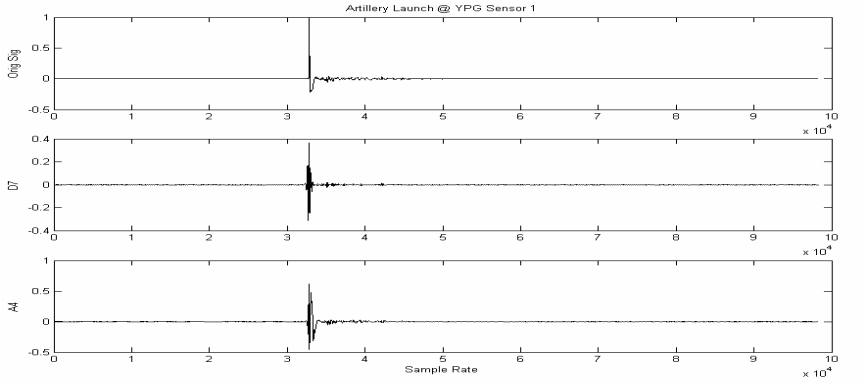

Figure 5b – Artillery Launch Signal and Wavelet Decomposition using db7 and db4 to produce details at level 7 and approximations coefficients at level 4 from Sensor 2.

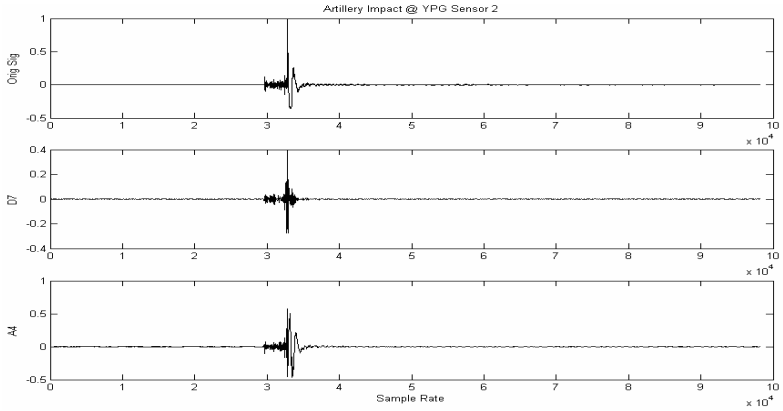

Figure 5c – Artillery Launch Signal and Wavelet Decomposition using db7 and db4 to produce details at level 7 and approximations coefficients at level 4 from Sensor 1.

Figure 6 (a-d) shows several permutations of 2-D subspaces for the entire set of YPG 1 test data used to train and initially benchmark the performance of a neural network classifier. An 'x' is used to indicate features derived from the impact event while the corresponding launch event feature points are depicted with an 'o'. Note that the resulting subspaces reveal a high degree of separability, notwithstanding the variability in the ranges at which data was acquired.

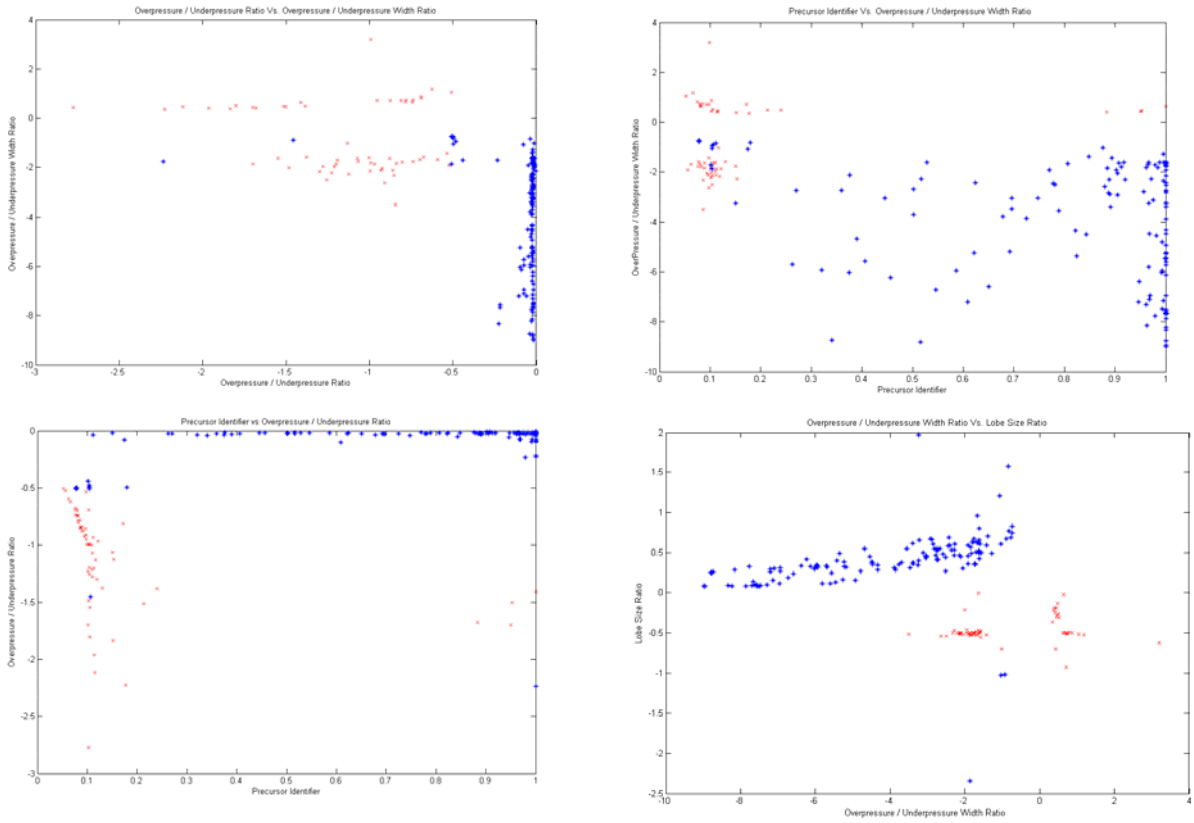

Figure 6 – 2D Feature Spaces derived from the YPG data set (a) $S_{pressure}$ vs. X_{width} (b) $S_{precursor}$ vs. X_{width} (c) $S_{precursor}$ vs. $S_{pressure}$ (d) X_{width} vs. $Y_{loberatio}$

3. NEURAL NETWORK CLASSIFIER

Neural networks have become a powerful tool for solving difficult classification (mapping) problems with a proven ability to realize non-linear discriminant functions and complex decision regions that are often required to ensure separability between classes. The use of neural networks for classification is well documented and convergence requirements for training are well known. The standard multilayer feedforward neural network shown in Figure 8 was chosen due to its ability to learn mappings of any complexity, provided that the number of hidden layer neurons is sufficient to accommodate the number of separable regions that are required to solve a particular classification problem. In general, the network contains N_i inputs, N_h hidden layer neurons and N_O output layer neurons with no interconnections within a single layer. In the three-layer network shown, the connection weight between the i^{th} input and j^{th} hidden layer neuron will be denoted as w_{ij} and v_{ij} will be used to denote the connection weight between the j^{th} neuron in the hidden layer and k^{th} output layer neuron. A bias for the j^{th} hidden layer neuron is denoted as b_j and the bias for the k^{th} output neuron is $\hat{b}_k$. x^p denotes the set of P, N-tuple feature vectors $x_n \in \Re^N$, $x^p = \left[x_1^p, x_2^p, \ldots, x_N^p\right]$ used to discriminate between the different classes of artillery.

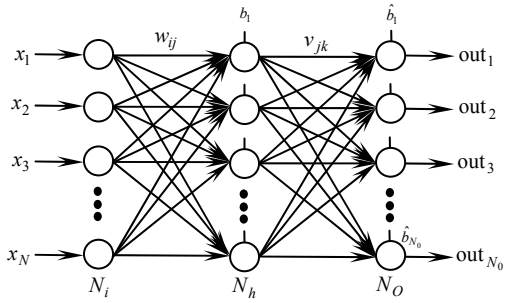

Figure 7– Standard Multilayer Feedforward Neural Network.

The input layer units or "neurons" propagate signals to the hidden layer but do not perform any computations. Neurons in the hidden layer and the output layer compute their response by taking a weighted sum signals from the previous layer plus a bias, and then passing the sum through an activation function. For example, the output of the j^{th} neuron in the hidden layer upon the presentation of the p^{th} input pattern x^p is given by $\text{out}_j^P = f\left(\text{net}_j^P\right)$ where $\text{net}_j^P = \sum_{i=1}^{N} w_{ij} x_i^P + b_j$, and f is an activation function, that was chosen to be the sigmoid function

$$f(net) = \frac{1}{1+e^{-net}} \qquad (9)$$

The neural network classifier used to discriminate between LA and IM artillery blasts was trained using the generalized delta rule or back propagation algorithm. The algorithm sequentially adjusts the interconnection weights within the network, subsequent to the application of all patterns in a training set, a routine commonly referred to as an epoch. In general, when an input pattern x^p from a training set is presented to the network, it produces and output that is different from the target value, say d^P. The error for the specific pattern is defined as the squared error $E_P = \frac{1}{2}\sum_{k=1}^{N_0}\left(d_k^P - \text{out}_k^P\right)^2$. An unconstrained nonlinear optimization is performed to minimize the total error function of the network

$$E(w) = \sum_{k=1}^{P} E_P(w) \qquad (10)$$

through the incremental computation of the gradient of the error in equation (9), and successive adjustment of the interconnection weights so as to achieve the global minimum error corresponding to $E(w) = 0$.

4. RESULTS

4.1 EXPERIMENT 1 RESULTS

Features were extracted from the data sets using the DWT as described in section 2, and the 5-tuple feature vector $\zeta^p = \left|F_{A4}^p, S_{firstpeak}^p, S_{pressureratio}^p, X_{widthratio}^p, Y_{peakratio}^p\right|$ was constructed according to equations (3), (4), (5), (6), and (7), respectively. Experiments were then conducted to measure the separability of the feature space and benchmark the performance of the proposed neural network classifier. The architecture of the neural network consisted of five hidden layer neurons trained using 20 randomly selected vectors

from a total of 177 signatures made available from the YPG exercise in March of 2005, YPG 1. The training set comprised of 10 samples of various mortars and artillery launches and 10 samples of corresponding impact events collected at each of the 2 sensor sites. When tested against the remaining 157 signatures, the networked correctly classified 97.6% of the impacts and misclassified a total of 3 out 115 (or 97.4%) of the remaining launch events, for an overall performance of 97.5%. The events were classified as an impact when the output from the sigmoid activation function in equation (9) was greater than ½ and launch otherwise.

Table 1 – Weights for a five hidden layer, single output neural network, trained using data from the YPG1 test and that provided 97.8% accuracy of classification against Launch / Impact signatures collected at YPG1.

w_{i1}	w_{i2}	w_{i3}	w_{i4}	w_{i5}	v_{j1}
-0.23395	0.47804	1.0611	1.4981	1.4981	-2.4532
0.18034	0.021191	0.72646	0.98692	0.29106	-0.52748
1.3601	0.77094	0.39468	-1.6406	-1.3085	-1.2209
-0.06934	0.48676	0.00798	1.9345	1.8651	5.8834
1.3549	0.58969	1.0702	-0.26853	-0.67183	4.6882
0.92314	0.76969	1.1339	-0.90694	-0.52655	-2.3007

Table 2 - Summary of the Classification Performance Results

Experiment #	Training Data	Test Data	Classification	Percentage
1	10 IM (YPG 1)	52 IM (YPG 1)	51 IM / 1 LA	98.1%
	10 LA (YPG 1)	125 LA (YPG 1)	122 LA / 3 IM	97.6 %

4.2 EXPERIMENT 1 RESULTS

A secondary data collection exercise was conducted in January 2006 at Yuma Proving Grounds. The purpose of this data collection was to test the original algorithm in a C++ environment and to extend distances for the data collection to see the effects of range from the acoustic source. Only Type D mortar rounds were fired. The resulting data analyses lead to the development of a 6th feature described in section 2.2 describing the initial excitation that the acoustic event wave carries prior to the main blast event. Our new resulting feature space, using the DWT as described in section 2, is a 6-tuple vector $\zeta^p = \left| F^p_{A4}, S^p_{firstpeak}, S^p_{pressureratio}, X^p_{widthratio}, Y^p_{peakratio}, E^p_{energy} \right|$ and is constructed according to equations (3), (4), (5), (6), (7), and (8). Following similar steps as explained within section 4.1 we trained a neural network with a total error less than 5e-3 and a learning rate of 0.1 for the back propagation algorithm. The data set comprised of all signatures collected at both data collection exercises conducted at YPG. The sensor layout for experiment 2 is described by figure 6. Four acoustic sensors were emplaced by the ACOE from ARDEC at sensor sites S1-S4 with ranges varying from 750m to 2000m from the firing position.

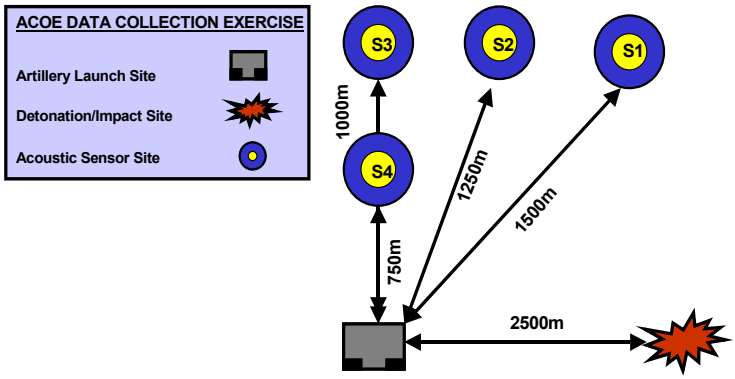

Figure 8 –Layout of Sensor Emplacement at Yuma Proving Grounds for Data Collection 2.

The results of the combined data sets tested against the new neural network are given by tables 3, 4 below and show some improvement on launches. This data was collected at much greater distances and a larger variety of variant rounds for discrimination of Launch/Impact events when compared to the initial data set. To increase the robustness of the feature space we developed an additional feature to ensure separability. The final overall classification is skewed with the data that is biased by the launches once correcting for the bias the current ability to classify events as either LA or IM from 6 varieties of artillery with distances varying from 300m to 2000m is 88% for 39 out of 52 IM events and 51 of 52 LA events.

Table 3 – Weights for a six hidden layer, single output neural network, trained using data from the YPG 1&2 tests and that provided 94.2% accuracy of classification against Launch / Impact signatures collected at YPG 1&2.

w_{i1}	w_{i2}	w_{i3}	w_{i4}	w_{i5}	w_{i6}	v_{j1}
1.0594	0.075848	0.22013	-0.3178	-0.06255	-0.24012	-2.3166
0.09456	0.74768	0.21807	1.4136	1.0502	1.1357	3.5142
0.50246	-0.93754	0.4027	-0.31275	-0.52205	-0.04328	-0.06704
-0.13517	1.1943	0.88895	1.558	1.4953	1.5777	4.2355
0.55117	-0.73524	-0.15725	-0.95844	-0.90025	-0.35321	3.3836
0.77674	2.213	0.40684	2.6697	2.2485	1.9433	2.3323
0.95667	-0.87471	0.79408	-0.42563	-0.37524	-0.03519	-4.3248

Table 4 - Summary of Classification Performance Results

Experiment #	Training Data	Test Data	Classification	Percentage
2	10 IM (YPG 1&2)	52 IM (YPG)	39 IM / 13 LA	75%
	10 LA (YPG 1&2)	241 LA (YPG)	237 LA / 4 IM	98.34 %

4.3 EXPERIMENT 3 RESULTS

A third data collection exercise was conducted between May 31st and June 1st 2006 at Yuma Proving Grounds. The purpose of this data collection was to further test the original algorithm in a C++ environment. Also the experiment was used to analyze the influence of range variance on sound propagation from the acoustic source and its affects the developed feature space. Only Type C mortar rounds were fired at this data collection exercise, with several varying factors including round temperature (hot, cold, normal operation), proximity fuse, impact detonation, and various ranges. Over the two-day data collection the assorted lots of Type C rounds were fired at various distances, ranging from 1000m-7500m. The air temperature was significantly higher from previous data collections, (100^0-106^0 Fahrenheit). Testing occurred under clear skies from the period of 0900-1500hrs. Figures 9 and 10 show the sensor deployment schemes for the two-day data collection are shown with approximate distances for the three acoustic sensors that were emplaced by the ACOE from ARDEC; S1, S2, and S3. The distances from the firing point and impact zones to the sensor sites are shown in figures 9 and 10.

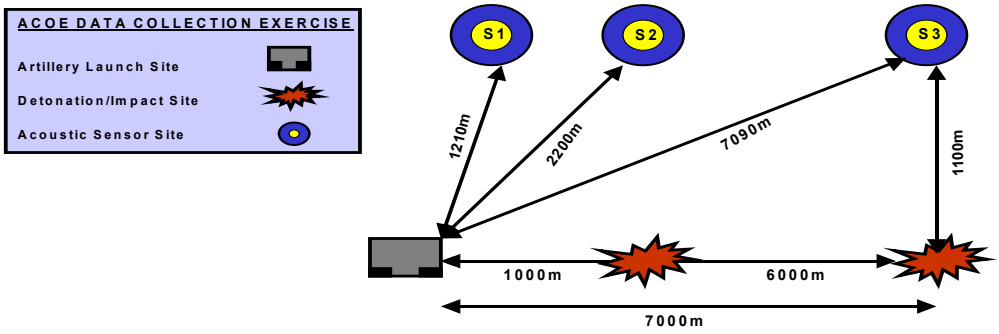

Figure 9 – Layout of Sensor Emplacement at Yuma Proving Grounds May 31st, 2006 for Data Collection 3.

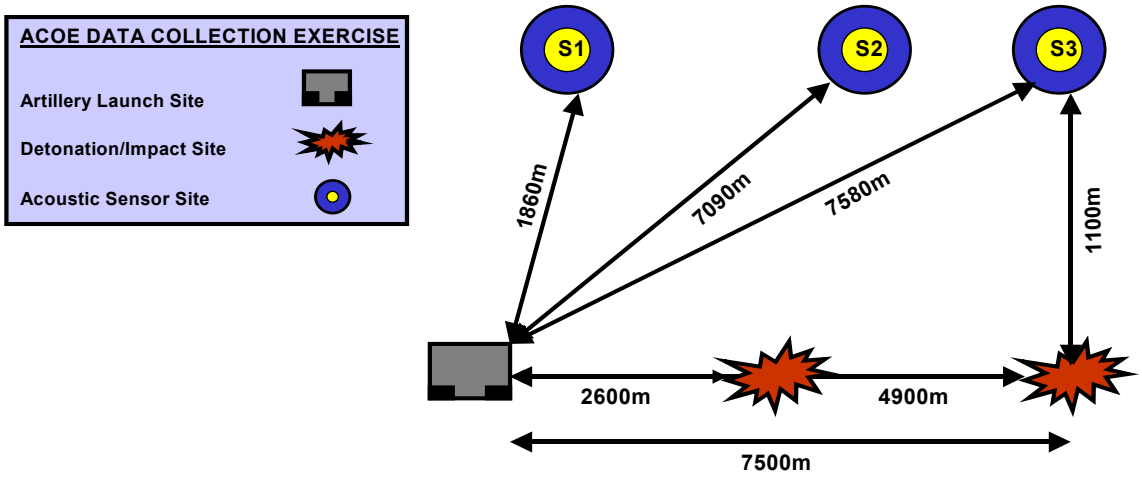

Figure 10 – Layout of Sensor Emplacement at Yuma Proving Grounds June 1st, 2006 for Data Collection 3.

Exploiting the neural network weights described in section 4.2 and utilizing the 6-tuple vector, $\zeta^p = \left| F^p_{A4}, S^p_{firstpeak}, S^p_{pressureratio}, X^p_{widthratio}, Y^p_{peakratio}, E^p_{energy} \right|$ constructed from equations (3), (4), (5), (6), (7), and (8) found in section 2.2 the acoustic events are discriminated as Launch or Impact. Shown in table 5 are results Experiment 3a from data collection 3, while experiment 3b is the results of the entire data population. The sample set has greater diversity of mortar and artillery variants. Sound propagation is directly affected by range and environment degrading the acoustic signal; however the feature space maintains a high level of separability. Collection exercise 3 reduces the disparity between launches and

impacts providing a more balanced data set for analysis. The numbers reflect the latest data, including acoustic detections in excess of 7000 meters. Propagation of acoustic signals is clearly affected at these extended ranges skewing the numbers of classification. Experiment 3 provided vital insight into the influence of distance on both signal propagation and the feature space.

Table 5 - Summary of Classification Performance Results

Experiment #	Training Data	Test Data	Classification	Percentage
3a	10 IM (YPG 1&2)	84 IM (YPG)	75 IM / 9LA	90%
	10 LA (YPG 1&2)	244 LA (YPG)	180 LA / 64 IM	74 %
3b	10 IM (YPG 1&2)	136 IM (YPG)	114 IM / 22LA	84%
	10 LA (YPG 1&2)	485 LA (YPG)	417 LA / 68 IM	86 %

5. CONCLUSIONS

In this paper, feature extraction methods based on the discrete wavelet transform and multiresolution analysis facilitate the development of a robust classification algorithm that affords reliable discrimination between artillery launch and impact events via acoustic signals produced during detonation of both the expulsion of the artillery round and explosion of the round payload upon impact. Previous methods for artillery event discrimination were based on visual cues rather then remote acoustic methods, which vary on proximity to the event and line of sight. Amplitude dependant features, which vary dramatically due to signal attenuation and distortion resulting from various propagation effects, are minimized through the use of signal processing techniques that exploit class specific attributes that remain constant within the signature data [6].

The non-stationary, transient and often oscillatory nature of artillery blast signals may be represented efficiently with wavelet bases that effectively capture the time-frequency distribution of such signal components. Wavelets are better suited for analyzing transient signals, as they are well localized in time and in frequency, and are able to take into account the scale of discrete signal components. To this end, the wavelet transform has been shown to provide a scalable time-frequency representation of blast signatures and has uncovered details that are not readily detectable using conventional signal processing techniques. Utilizing the idea of multiresolution analysis provided by the discrete wavelet transform, we were able to break the original signature into subband components thereby removing the higher frequency noise features and creating two sets of coefficients at varying levels of decomposition. These coefficients are obtained each time the signal is passed through a lowpass and highpass filter bank whose impulse response is derived from Daubechies db4 and db7 wavelet, as well some elements of the original signature. Distinct features are obtained through the process of isolating the details of the higher oscillatory components of the signature (i.e. characteristic whining of the shrapnel for IM rounds and weak under pressure for LA rounds).

The discrete wavelet transform has been successfully employed to extract distinct, disjoint feature sets that remain consistent for a given class of round and do not degrade dramatically with long-range propagation. Classification results using a neural network trained on the feature set show reliable discrimination of artillery launch and impact events. Discrimination exceeds 88% for events less then 4000 meters from the acoustic sensor, while 74% for events between 4000 - 7500 meters. The initial part of the paper demonstrates the effectiveness of wavelets to discriminate Launch and Impact events. The final section illustrates the effectiveness of wavelets against the affects of signal degradation from long-range propagation sustaining reliable discrimination of launch/impact events for artillery and mortar rounds.

REFERENCES

[1] H.E. Bass, ”Aero Acoustic Blast Classification Study (ACBS)”, Interim Report for contract 95-F139300-000, January, 1996

[2] Birenzvige, A., Sickenberger, D., and Reyes, F., “Disparate Sensor Integration Program Description and Preliminary Data Analysis”, Report ECBC-TR-251, Edgewood Chemical Biological Center, September 2002.

[3] Daubechies, I., 1992, Ten Lectures on Wavelets: SIAM, Capital City Press.

[4] Vetterli, M., Kovacevic, J., “Wavelets and Subband Coding”, Prentice Hall, NJ 1995

[5] Mallet, S., “A theory for Multiresolution Signal Decomposition: The Wavelet Representation.”, IEEE Transactions on Pattern Analysis and Machine Intelligence, Vol. 11. No. 7. July 1989.

[6] Hohil, M., Desai, S., Chang, J., “Discrimination between High Explosive and Chemical/Biological Artillery Using Acoustic Sensors.” Military Sensing Symposia, Laurel, MD. August 2004.

Classifying Launch/Impact Events of Mortar and Artillery Rounds Utilizing DWT Derived Features and Feedforward Neural Networks

US Army RDECOM-ARDEC

By: Dr. Myron Hohil, Mr. Sachi Desai, and Mr. Amir Morcos

Outline

- Purpose, motivation for work.
- Data collection exercise 1, and results.
- Data collection exercise 2, and results.
- Data collection exercise 3,results and benchmarking algorithm.
- Conclusion and closing remarks.

Motivation and Purpose

- ARMY is currently developing Acoustic Sensor Systems for battlefield surveillance.
- Acoustic blast waves from artillery events introduces a feature for using acoustics for the early detection, localization, and identification of explosive events i.e impacts (IM) and launches (LA).
- This added information integrated into the **Decision Aide** will
  - Allow a field commander to make **rapid and accurate judgments** that insure greater safety and lessen exposure for the soldiers.
  - Could help **reduce the time-consuming, manpower intensive** and dangerous tasks associated with identifying artillery events.
- Our work is intended to promote the reliability associated with using acoustic sensor technologies to discriminate between Artillery (LA) and Artillery (IM) using features that remain robust with artillery variants.

Experiment/Test 1

Event (LA/IM), Data Collection #1

- Proving Ground Data Collection.
  - Conducted by ARDEC in cooperation with PM Mortars.
  - Type A, Type B, Type C, Type D, and Type E High Explosive rounds fired for a total of 177 launches and impacts signatures.
  - 125 Launch Events.
    - 20 (Type A), 25 (Type B), 30 (Type C), 16 (Type D), 34 (Type E) rounds
  - 52 Impact Events.
    - 4 (Type B), 26 (Type C), 22 (Type E) rounds.

Data Exercise #1 Layout

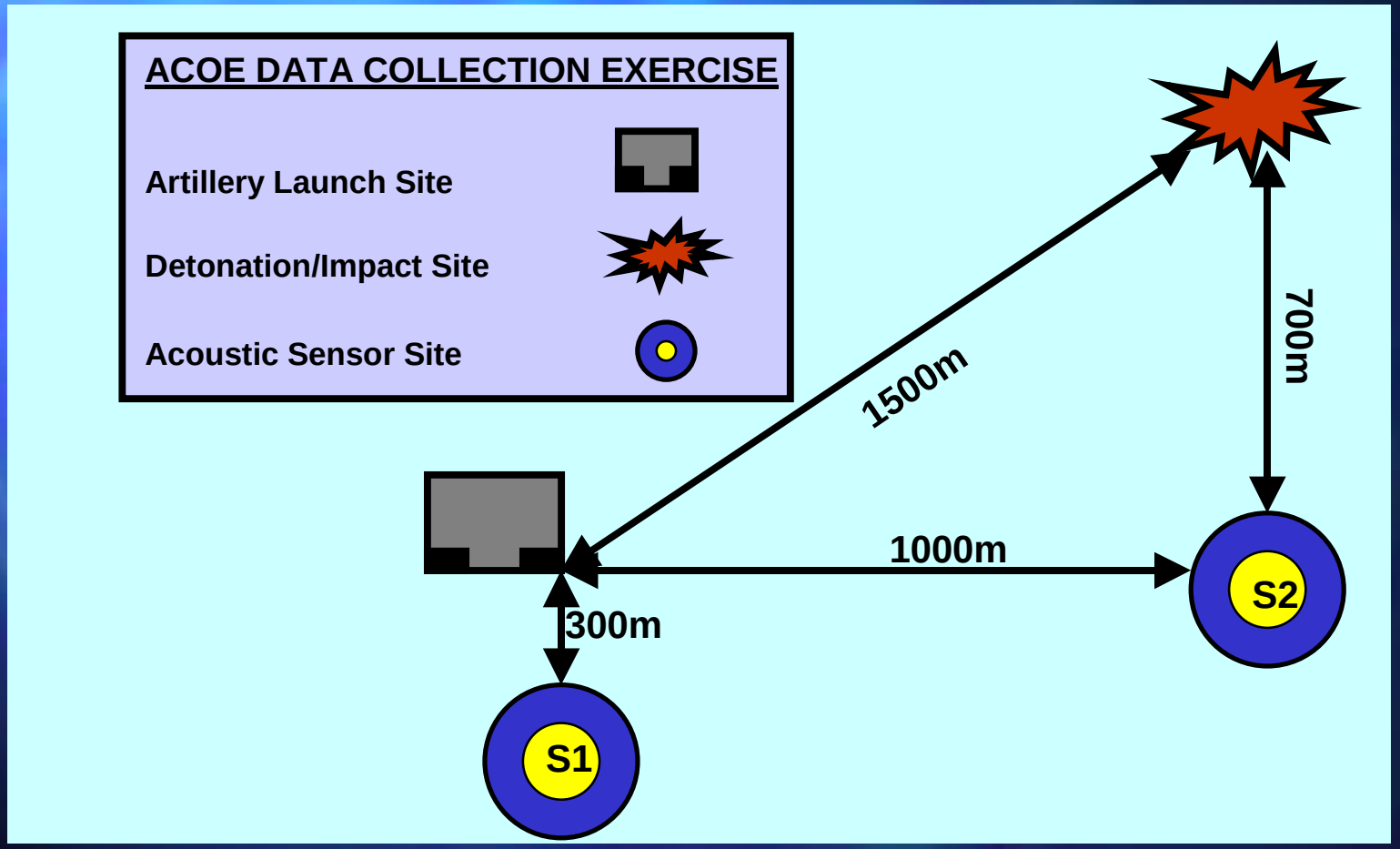

Typical Artillery Variant Launches and Impacts

- **Fig A.** A typical launch recorded from sensor site 1. The Launch clearly exhibits no activity energy prior to blast event.
- **Fig B.** A typical impact recorded from sensor site 2. The Impact displays activity prior to the main blast with an under pressure comparable to the overpressure.

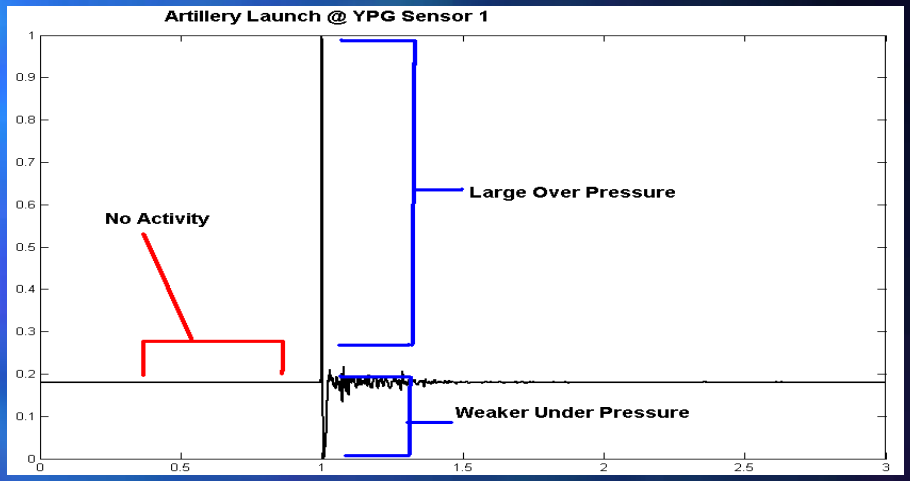

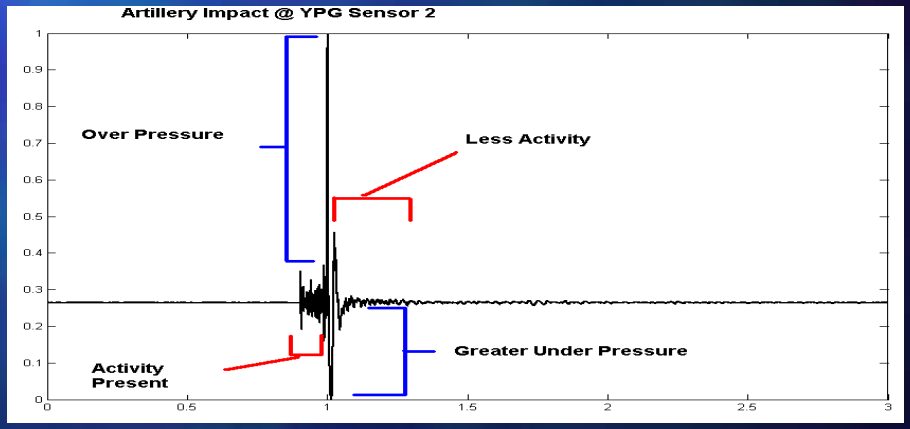

Discrete Wavelet Transform (DWT)

- Derived from subband filters and multiresolution decomposition.
  - Coarser Approximation.
  - Removing high frequency detail at each level of decomposition.
- Acts like a multiresolution transform.
  - Maps low frequency approximation in coarse subspace high frequency elements in a separate subspace.

Defining Parameters

Scaling Function

$$\phi(x) = 2^{1/2} \sum_{k=0}^{L-1} h_{k+1} \phi(2x - k)$$

Wavelet Function

$$\psi(x) = 2^{1/2} \sum_{k=0}^{L-1} g_{k+1} \phi(2x - k)$$

Daubechies Wavelet db(j), j = 4 and 7

- Efficiently represent non-stationary, transient, and oscillatory signals.
- Provide a scalable time-frequency representation of artillery blast signature.
- Representation of the scaling and translation function of db4 and db7.
  - Scaling function (a) and (c) resembles blast signature of artillery variants.
  - Provides the ability to approximate signal with the characteristic wavelet.

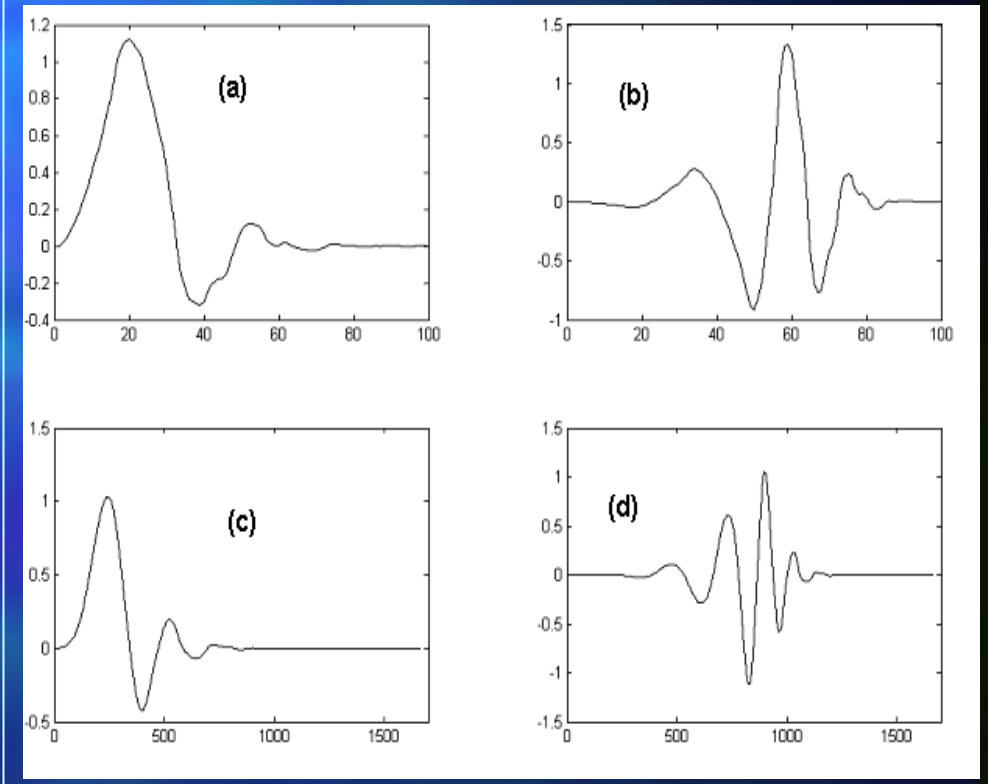

Multiresolutional Analysis

- Using a series of successive high pass and low pass filters to create a set of subspaces.
  - High pass filter obtains the details of the signatures while the low pass filter obtains a coarse approximation of the signal.
- The resulting banks of dyadic multirate filters separate the frequency components into different subbands.
  - Each pass through gives you resolution of factor 2.

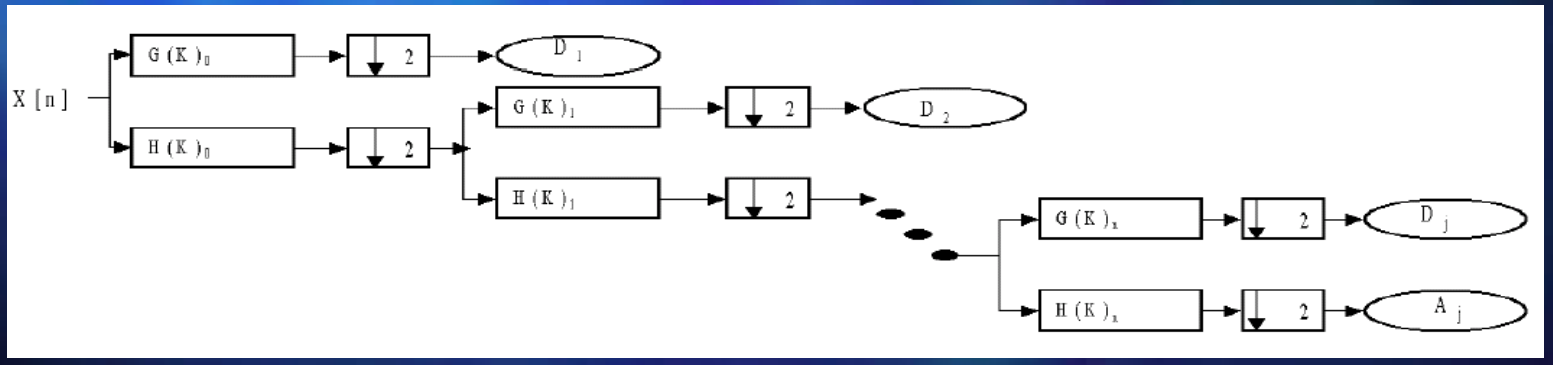

Effects of Wavelet Decomposition

- Wavelet decomposition to level 4 using db4 and level 7 using db7 of three artillery event types from varying ranges.

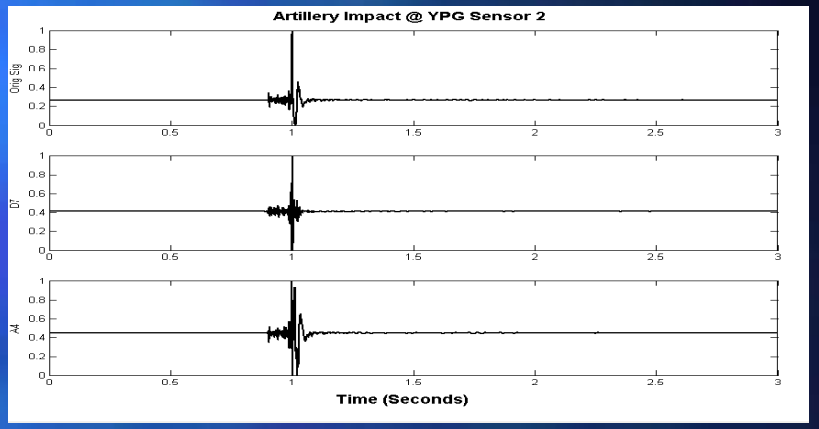

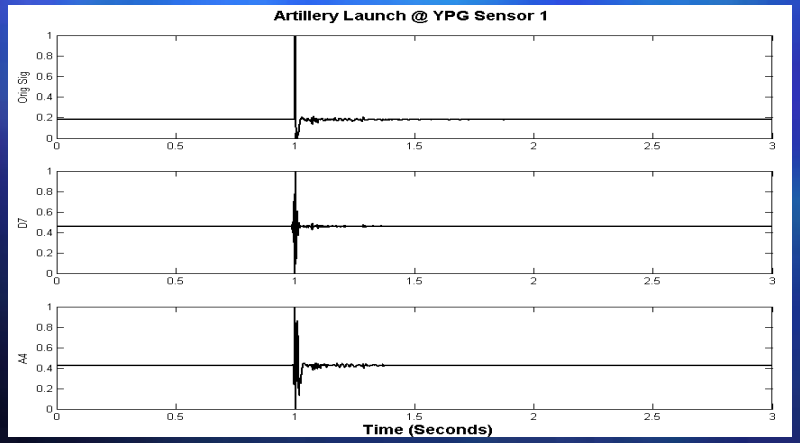

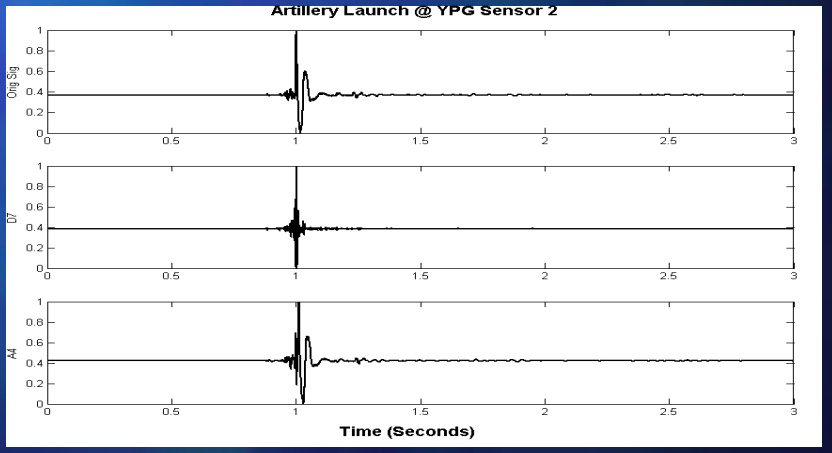

5-tuple Feature Space

- Analysis with the DWT leads to the discover of 5 distinct characteristics, amplitude independent describing an artillery event.
- The n-tuple representation of the acoustic signal becomes a 5-tuple space,

$$\zeta^p = \left| F^p_{A4}, S^p_{firstpeak}, S^p_{pressureratio}, X^p_{widthratio}, Y^p_{peakratio} \right|$$

, applied for classification.

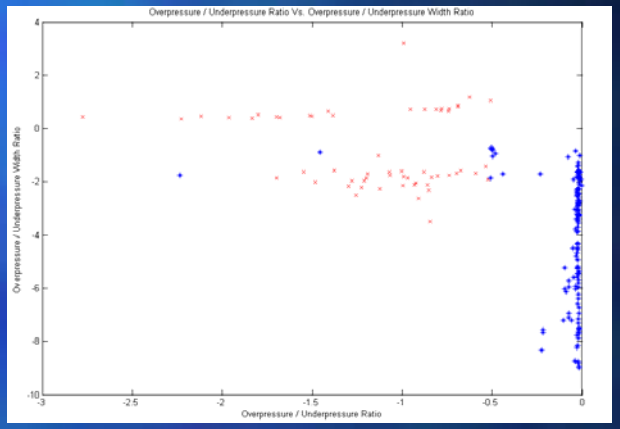

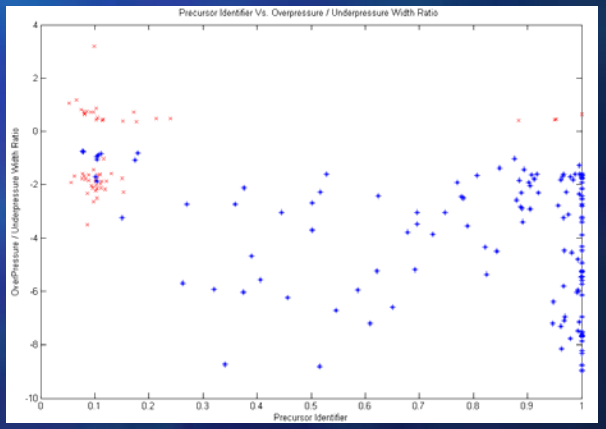

Neural Network

- Realize non-linear discriminant functions and complex decision regions to ensure separability between classes.
- Standard Multilayer Feedforward Neural Network.
- Number of hidden layer neurons depend on complexity of required mapping.

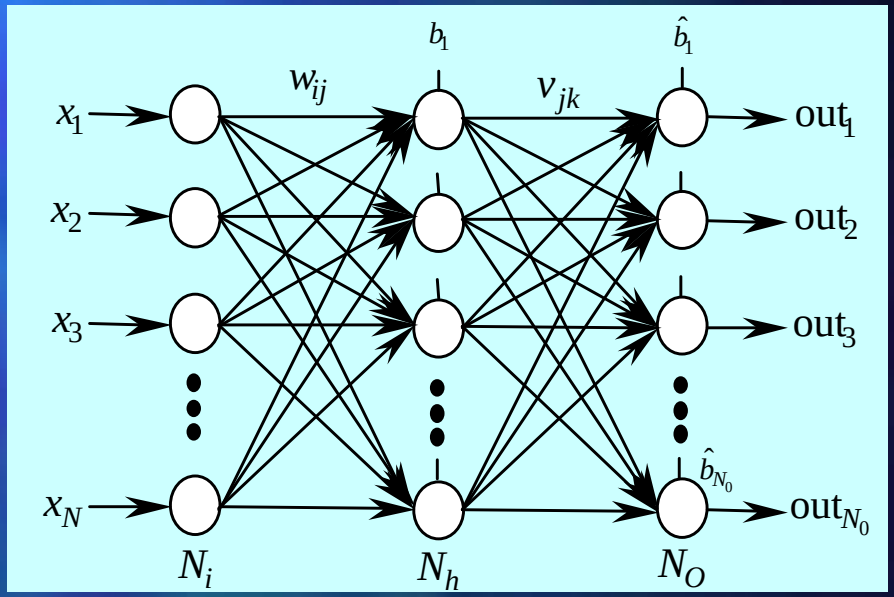

Results of LA/IM Discrimination Experiment #1

- Experiment 1 Results:
  - 98.1% Impact Discrimination
  - 97.6% Launch Discrimination
  - 97.7% Overall Discrimination
  - **97.8%** Weighted Discrimination

w_{i1}	w_{i2}	w_{i3}	w_{i4}	w_{i5}	v_{j1}
-0.23395	0.47804	1.0611	1.4981	1.4981	-2.4532
0.18034	0.021191	0.72646	0.98692	0.29106	-0.52748
1.3601	0.77094	0.39468	-1.6406	-1.3085	-1.2209
-0.06934	0.48676	0.00798	1.9345	1.8651	5.8834
1.3549	0.58969	1.0702	-0.26853	-0.67183	4.6882
0.92314	0.76969	1.1339	-0.90694	-0.52655	-2.3007

Experiment	Training Data	Test Data	Classification	Percentage
1	10 IM (Ex. 1)	52 IM (Ex. 1)	51 IM / 1 LA	98.1%
	10 LA (Ex. 1)	125 LA (Ex. 1)	122 LA / 3 IM	97.6%

Experiment/Test 2

Event (LA/IM), Data Collection #2

- Proving Ground Data Collection.
  - Conducted by ARDEC in cooperation with PM Mortars.
  - Type F Illumination rounds fired for a total of 116 launches and impacts signatures.
  - 116 Launch Events.
  - Greater Variety of Distances testing limitations of features.

Data Exercise #2 Layout

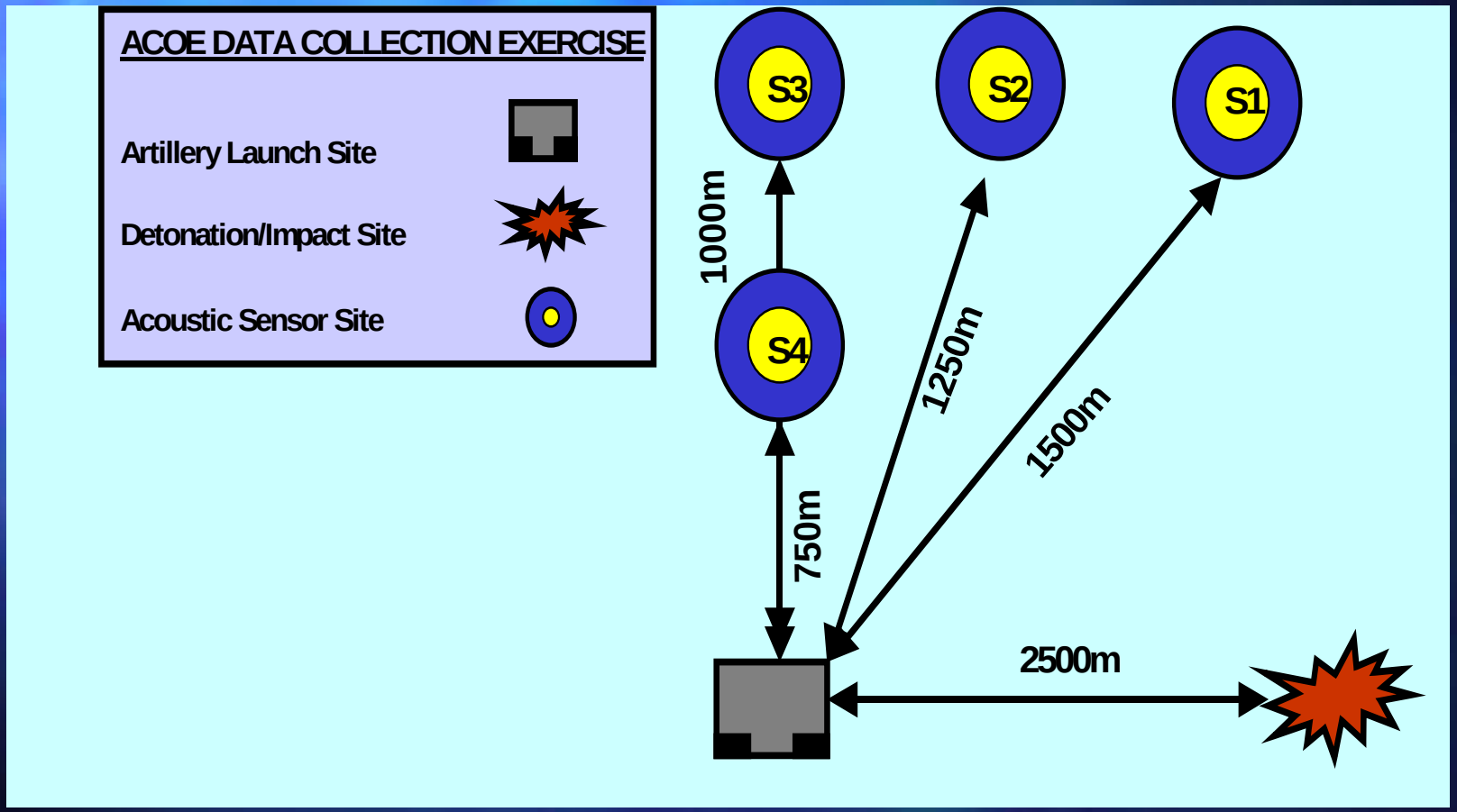

Refined Feature Space

- 2nd Data collection lead to refinement of feature space.
- Feature space expanded to 6-tuple element.
- An amplitude independent feature based on the characteristics associated with explosion of the variant artillery.
- The 2 data collection exercises encompass now 6 artillery/mortar variants (HE & Illum.) and distances ranging from 300m to 2000m.

$$\zeta^{p} = \left| F^{p}_{A4}, S^{p}_{firstpeak}, S^{p}_{pressureratio}, X^{p}_{widthratio}, Y^{p}_{peakratio}, E^{p}_{energy} \right|$$

Extracted Features Comprising the n-tuple Vector

- The count of the prominent frequencies in the A4 subband. F_{A4}^{p}
- A major precursor peak to the defined main blast event. $S_{firstpeak}^{p}$
- Distribution of blast energy within overpressure and underpressure in the A4 subband. $X_{widthratio}^{p}$
- The magnitude of the overpressure vs. the underpressure of the main blast event. $S_{pressureratio}^{p}$
- The energy contained within the wave prior to the main blast event. E_{energy}^{p}
- The distribution of prominent peaks within the overpressure and underpressure. $Y_{peakratio}^{p}$

2-D Feature Space Realization

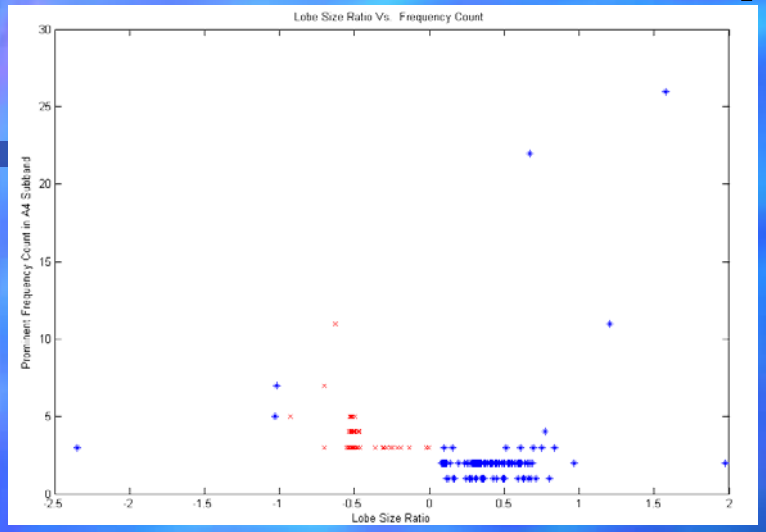

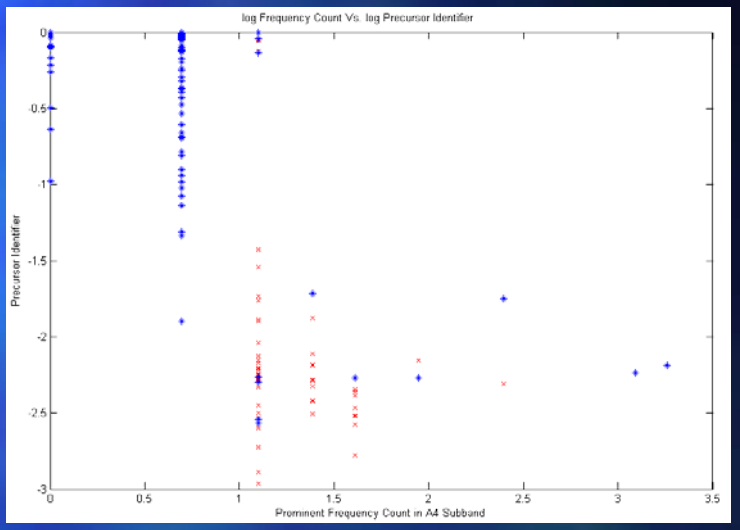

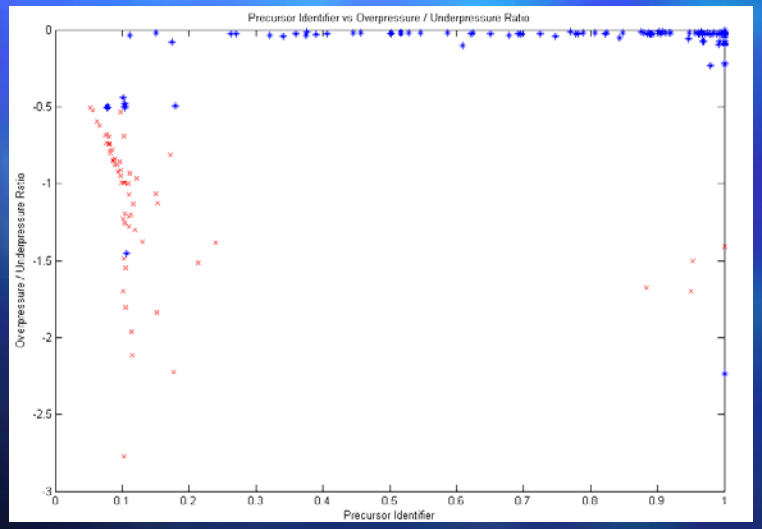

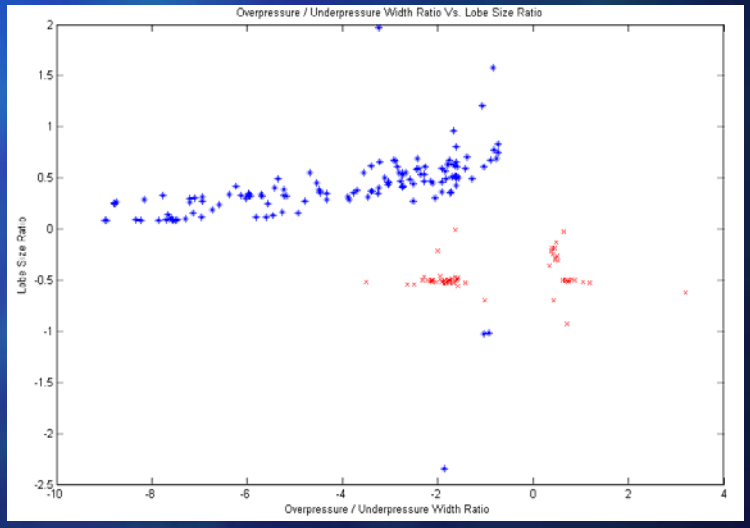

Results of LA/IM Discrimination Experiment #2

w_{i1}	w_{i2}	w_{i3}	w_{i4}	w_{i5}	w_{i6}	v_{j1}
1.0594	0.075848	0.22013	-0.3178	-0.06255	-0.24012	-2.3166
0.09456	0.74768	0.21807	1.4136	1.0502	1.1357	3.5142
0.50246	-0.93754	0.4027	-0.31275	-0.52205	-0.04328	-0.06704
-0.13517	1.1943	0.88895	1.558	1.4953	1.5777	4.2355
0.55117	-0.73524	-0.15725	-0.95844	-0.90025	-0.35321	3.3836
0.77674	2.213	0.40684	2.6697	2.2485	1.9433	2.3323
0.95667	-0.87471	0.79408	-0.42563	-0.37524	-0.03519	-4.3248

93.84% Overall Discrimination

75% Impact Discrimination

98.34% Launch Discrimination

86.67% Weighted Discrimination

Experiment	Training Data	Test Data	Classification	Percentage
2	10 IM (Ex. 1 & 2)	52 IM (Ex. 1 & 2)	39 IM / 13 LA	75%
	10 LA (Ex. 1 & 2)	241 LA (Ex. 1 & 2)	237 LA / 4 IM	98.34%

Experiment/Test 3

Event (LA/IM), Data Collection #3

- Data Collection 3.
  - Conducted by ACOE in cooperation with ARDEC.
  - Type C, High Explosive rounds fired for a total of 949 launches and impacts signatures.
  - 729 Launch Events and 220 Impact Events.
  - Greater Variety of Distances testing features vs. sound propagation and degradation.

Data Exercise #3a Layout

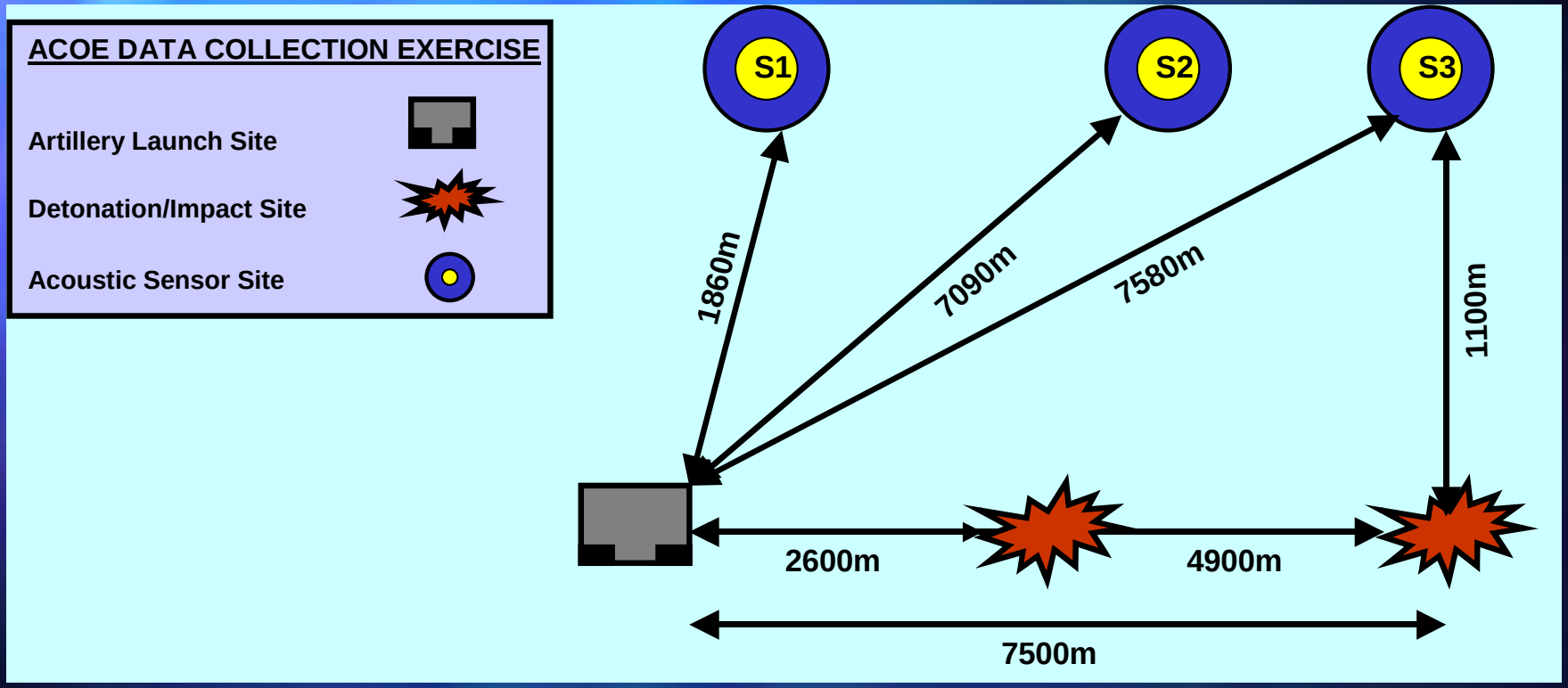

Data Exercise #3b Layout

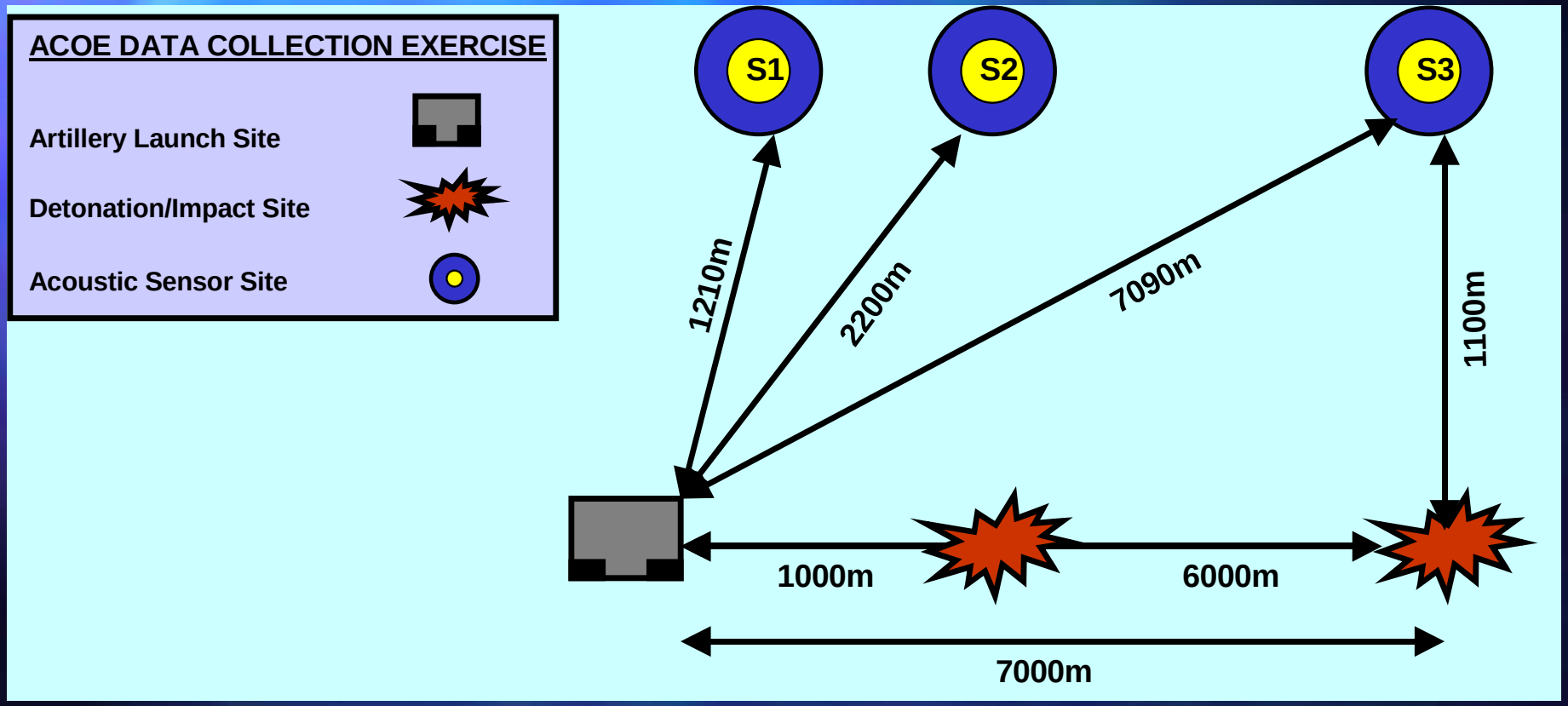

Summary Of Experiment 3 Discrimination

$$\zeta^{p} = \left| F^{p}_{A4}, S^{p}_{firstpeak}, S^{p}_{pressureratio}, X^{p}_{widthratio}, Y^{p}_{peakratio}, E^{p}_{energy} \right|$$

Experiment	Training Data	Test Data	Classification	Percentage
3a	10 IM(Ex.1 & 2)	84 IM	75 IM / 9 LA	90%
	10 LA(Ex.1 & 2)	244 LA (YPG)	180 LA / 64 IM	74%
3b	10 IM(Ex.1 & 2)	136 IM (YPG)	114 IM / 22LA	84%
	10 LA(Ex.1 & 2)	485 LA (YPG)	417 LA / 68 IM	86%

Conclusion

- Features extracted facilitate robust classification.
  - **Using DWT and Multiresolutional Analysis.**
  - **Reliable discrimination of LA events, 98.3%, d>2000m.**
  - **Reliable discrimination of LA/IM events, 86%, d>7000m.**
  - **6 variants** of artillery and mortars.
  - Varying **weather** conditions, **seasons**, and **times of day**.
- Completed implementation of algorithm into C++ environment for real-time processor.
- The features this algorithm is based on go beyond previous amplitude dependent features.
  - Detonation point to acoustic sensor exceed visual sight and LOS, **greater then 4km**.
  - Degradation due to signal attenuation and distortion is nullified/minimized.
- Scalable time frequency representation uncovered non-readily detectable features.
- Furthering Research
  - Variant Classification, ability to classify type of artillery or mortar round i.e. caliber based on acoustic based feature set.
  - Extend data set to include more impact recording with future tests.
  - Extend bound of sensors from zones of interest.
- Future Considerations.
  - Networking of sensors can provide TDOA abilities to further **localize a threat**.
  - Integration into existing artillery and mortar event detection systems to provide further Situational Awareness.

QUESTIONS..?

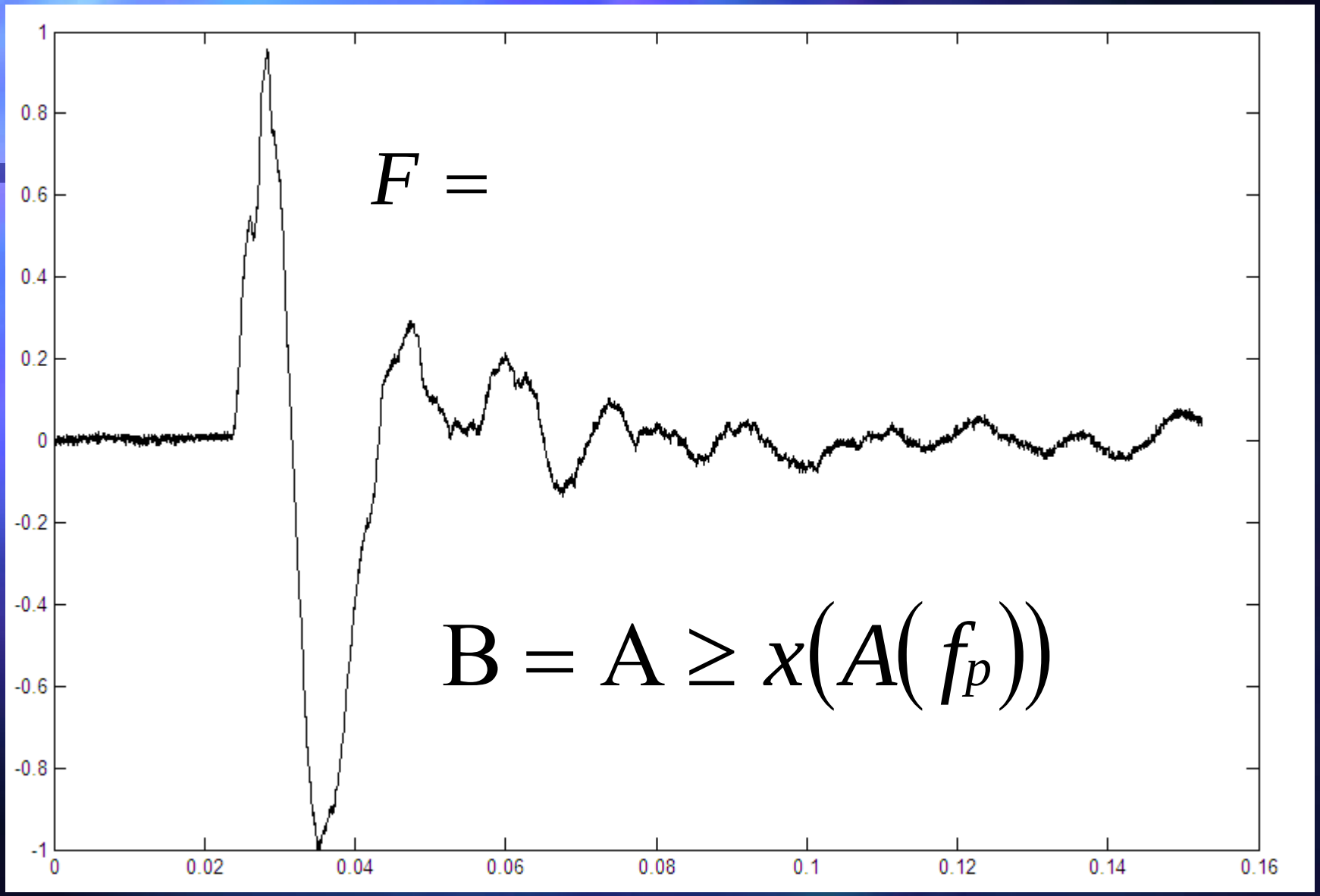
F =
B = A ≥ x(A(fp))
1
0.8
0.6
0.4
0.2
0
-0.2
-0.4
-0.6
-0.8
-1
0
0.02
0.04
0.06
0.08
0.1
0.12
0.14
0.16

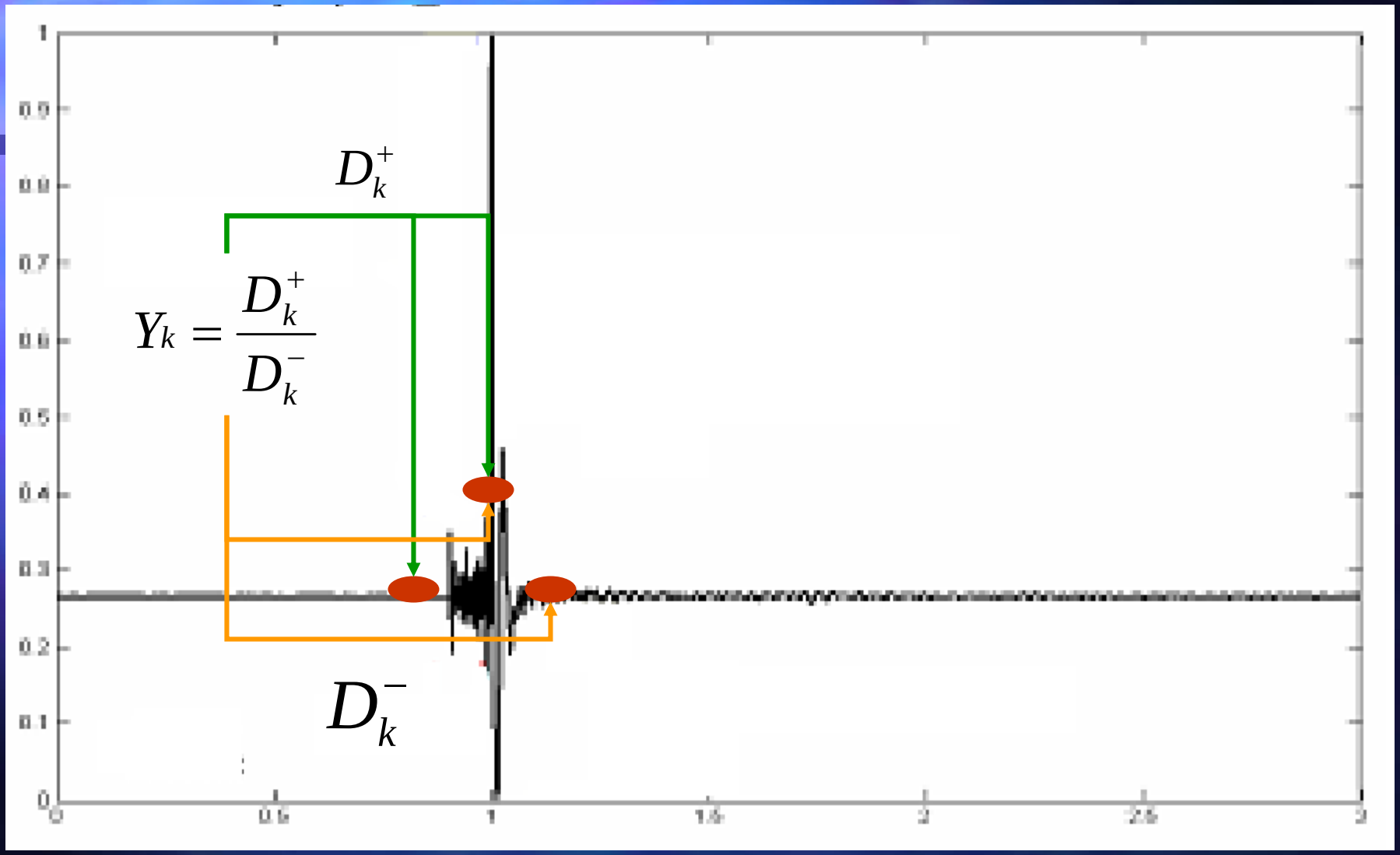
D_k^+
$Y_k = \frac{D_k^+}{D_k^-}$
D_k^-

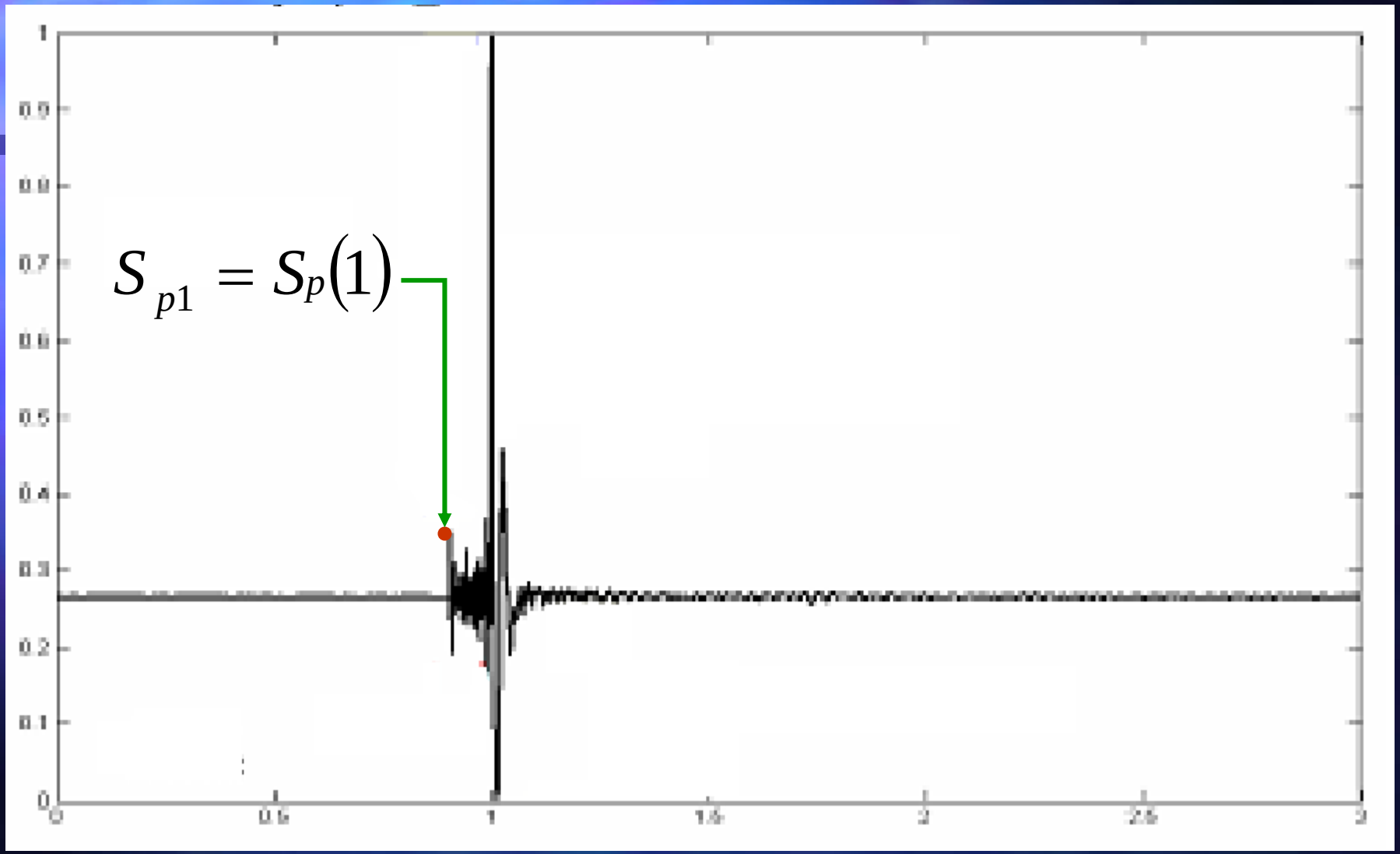
$S_{p1} = S_p(1)$

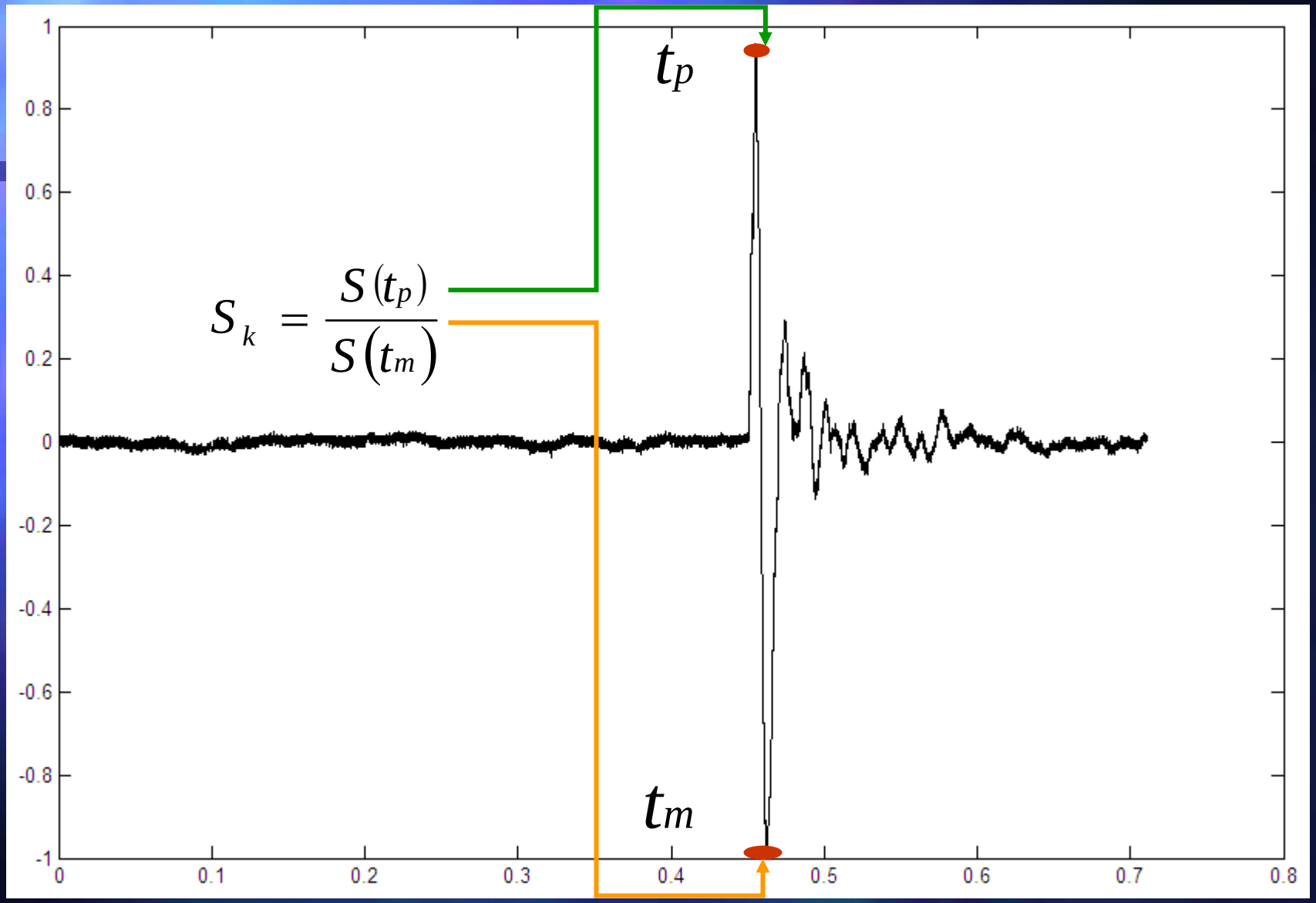
t_p
$S_k = \frac{S(t_p)}{S(t_m)}$
t_m
1
0.8
0.6
0.4
0.2
0
-0.2
-0.4
-0.6
-0.8
-1
0
0.1
0.2
0.3
0.4
0.5
0.6
0.7
0.8

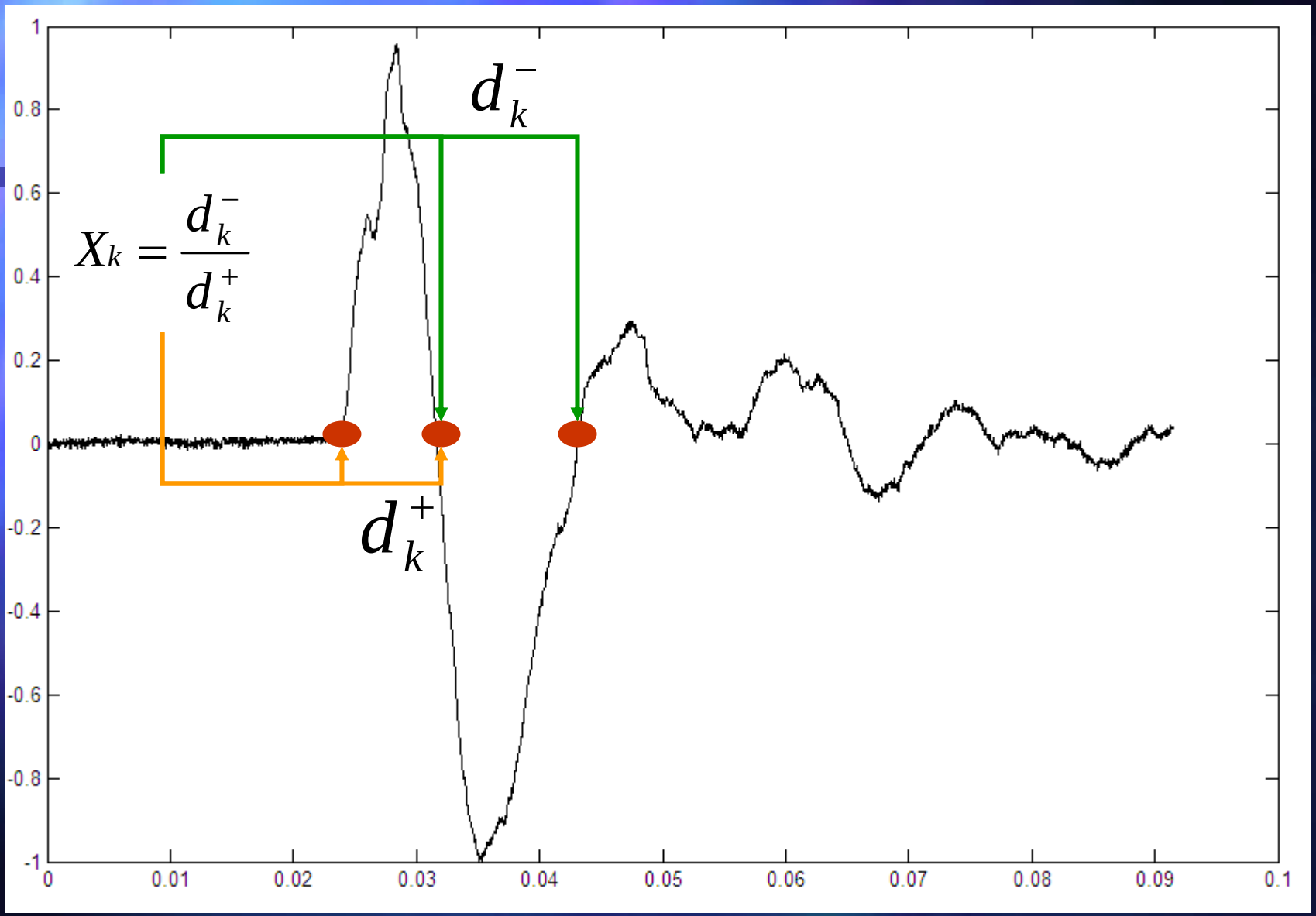
d_k^-
$X_k = \frac{d_k^-}{d_k^+}$
d_k^+
1
0.8
0.6
0.4
0.2
0
-0.2
-0.4
-0.6
-0.8
-1
0
0.01
0.02
0.03
0.04
0.05
0.06
0.07
0.08
0.09
0.1

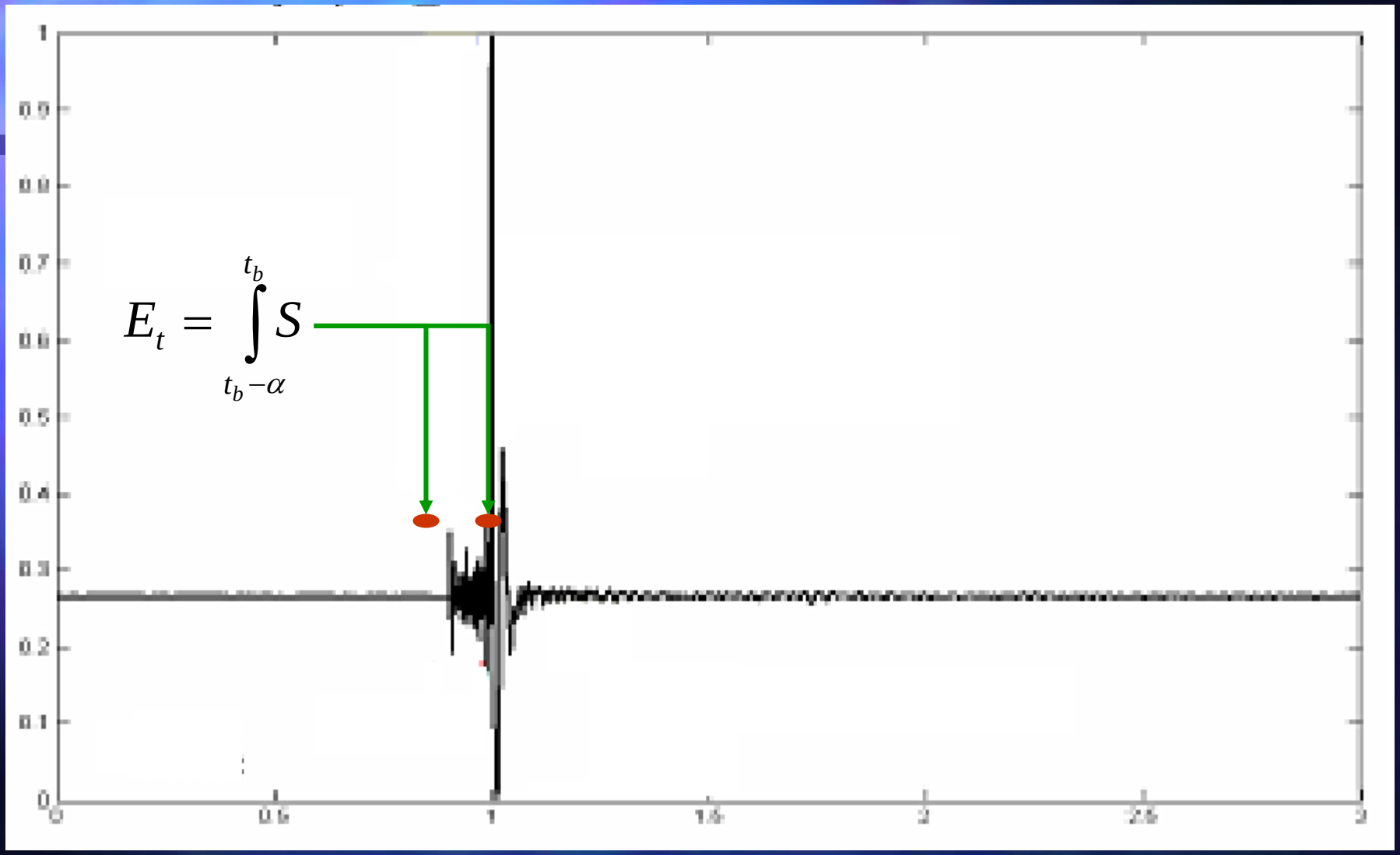
$E_t = \int_{t_b-\alpha}^{t_b} S$

BACK UP SLIDES/EXTRAS